

In-situ flash X-ray observation of impact crater formation in porous gypsum

YASUI, Minami^{1*}, ARAKAWA, Masahiko², HASEGAWA, Sunao³, FUJITA, Yukihiro⁴, KADONO, Toshihiko⁵

¹Organization of Advanced Science and Technology, Kobe University, ²Graduate School of Science, Kobe University, ³Japan Aerospace Exploration Agency, ⁴Graduate School of Environmental Studies, Nagoya University, ⁵Institute of Laser Engineering, Osaka University

Introduction: In order to understand the impact histories related to the asteroid formation processes, it is very important to study the impact craters found on the surfaces of asteroids. So, we should study the crater formation mechanism and establish the formation theory of the impact crater based on the physical mechanism. From recent spacecraft explorations, many asteroids were found to have low density and be porous bodies [1]. Porosity has an important effect on the crater formation: the void spaces were crushed due to impact pressure and the large craters with a compaction layer below the surface were formed [2]. So, the crater formation mechanism on the porous materials is important to understand the impact history of asteroids. The target internal structure changing with time during the crater formation process has not been studied yet by laboratory experiments because it is difficult to observe the target interior by visible light. In some previous works, impact experiments were conducted by using the porous transparent silica aerogel to visualize the target interior [3]. In this study, we tried to visualize the interior of the target during the crater formation process by using a flash X-ray generator and studied the elementary processes of the crater formation, and observed the projectile penetration and the cavity expansion in the target.

Experimental method: We prepared the targets of porous gypsum having cylindrical shape with two different diameters of 34 and 64 mm. Impact experiments were conducted by a two-stage H₂-gas gun in ISAS/JAXA. The impact velocities were 1.9-2.4 km/s (low-velocity) and 5.4-6.1 km/s (high-velocity) by using three types of projectile, stainless spheres with diameters of 1.6 and 3.2 mm, and Al sphere with 3.2 mm. We set two flash X-ray generators to take two images at different times for one test. Multiple images were obtained from several tests at the same impact condition and the different trigger timing from 0 to 250 micron-s.

Results: From the analysis of X-ray images, we found that the crater shape of target depended on the impact velocity and the projectile type. In the case of low-velocity collisions, the stainless projectile penetrated through the target without deformation and the penetrated hole was formed while the Al projectile collided the target surface and the hemispherical cavity was formed. In the case of high-velocity collisions for stainless projectile, the projectile with a diameter of 3.2 mm deformed and the hemispherical cavity was formed in the target, accompanied with some narrow pits on the cavity front. When the projectile with 1.6 mm collided, the hemispherical crater was formed on the surface. We measured the penetration depth (d), cavity diameter on the target surface (D) and the maximum diameter in the target (D_{max}). In the case of penetration hole, the D was almost constant for projectile diameter while the d increased with time exponentially. In the cases of hemispherical cavity, all parameters increased with the time until 20 micron-s, however, the increases of d and D_{max} stopped at 20 micron-s. Beyond 60 micron-s, the behavior depended on the stainless projectile size. In the case of small projectile, the D became the maximum and the spalling occurred on the target surface. In the case of large projectile, the d increased due to the progress of some disrupted projectiles. Conclusively, all parameters increased because the target was disrupted and many fragments were ejected. We examined the drag coefficient (C_d) of projectile by using the deceleration model [3], and found that the C_d for penetration was about 0.9 while that for other cases was about 2-3. This high value might be caused by the deformation of projectiles [4].

Reference: [1] Veverka *et al.* (1999), *Icarus* 140, 3-16. [2] Housen and Holsapple (2003), *Icarus* 163, 102-119. [3] Niimi *et al.* (2011), *Icarus* 211,986-992. [4] Tamaki and Hinada (1966), *Seisankenkyu* 18, 219-221.

Keywords: impact crater, penetration, pit, drag coefficient, flash X-ray, H-gas gun

The effects of multiple impacts on the impact strength of ice targets

HAYAMA, Ryo^{1*}, ARAKAWA, Masahiko¹

¹Graduate School of Science, Kobe University

High velocity collisions among icy bodies played an important role in the formation and the evolution of icy planets, icy satellites and KBOs. Actual icy bodies could have experienced multiple-impacts events however most of studies were single-impact experiments rather than multiple ones. In the previous studies related to multiple impacts experiments (Gault et al., 1969; Housen, 2008), it has been reported that cracks induced by pre-impacts have reduced the impact strength of targets. Furthermore, in their experiments, they changed the number of impact times using the same target and the sum of each impact energy in the same set of the experiment was always constant for each target. And, they found that the relationship between the largest fragments and the cumulative energy densities was consistent with that of single-impact experiments. The cracks formed by each impact are not distributed homogeneously in the target. Thus, in the multiple-impacts experiments, it is necessary to quantify the crack density inside the target generated by the pre-impacts. Then, we conducted multiple-impacts experiments to reveal the quantitative relationship between the pre-crack distribution and the impact strength.

Impact experiments were conducted using gas gun installed in a cold room at the Institute of Low Temperature Science, Hokkaido University. An ice projectile was impacted at several times (1 to 4) on the same target, and each impact was conducted on the different surface. The temperature was -10 deg C in the cold room. The impact velocity was from 140 to 480km/s. The projectiles had a cylindrical shape and the mass was 1.6 g. The target was cube made of polycrystalline water ice, and the mass was from 240 to 1280 g. To quantify the crack density of the recovered targets we measured P and S wave velocities of the target when they were not disrupted catastrophically. Then, in the next impact experiment, we used it again.

We changed the energy density (Q) of the first shot of each target, and the second shot were done at the same Q. From this experiment, in the case of high Q at the first shot, m_L/M , which is the largest fragment mass normalized by the initial target mass (M), became smaller. Thus, we found that m_L/M of pre-impact targets was much smaller than m_L/M of the previous results derived from the single-impact of icy projectile on ice target (Arakawa et al., 2002). These results suggest that the pre-cracks reduce the target strength, and moreover this mean that the relationship between the pre-cracks and the target strength strongly depends on the impact record of the target. On the other hand, the size distribution of fine fragments whose m/M , the fragment mass normalized by M, were less than 10^{-4} , was constant regardless of the number of impacts. This suggests that there is a lower limit of the fragment size affected by the pre-crack.

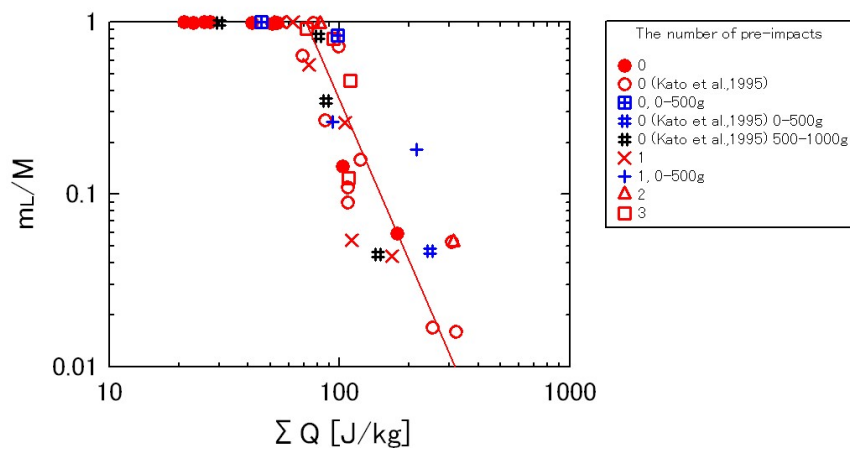
Furthermore, the relationship between m_L/M and sigma Q (the sum of Q for all impacts) for the targets which experienced multiple-impacts was consistent with that for the intact ice targets. Figure 1 shows the relationship between m_L/M and sigma Q. The vertical axis means the m_L/M and the horizontal axis means sigma Q, and each mark is classified by the number of pre-impact times. In this figure, the value of m_L/M depends on sigma Q, and the pre-impact and the target mass have few effects on m_L/M . These data were fitted by a power law equation and we obtained the empirical formula described by $m_L/M=7.8 \text{ times } 10^5 Q^{-3.2}$.

Elastic wave velocities for the recovered targets were measured and they were found to decrease with the increase of the crack density, and this relationship was theoretically discussed by O'Connell and Budiansky (1974) and they showed the theoretical equation showing the relationship between the crack density and an elastic body. By using this equation in this study, we found that the crack density linearly increased with sigma Q regardless of the number of impacts

PPS21-02

Room:201A

Time:May 21 15:45-16:00



Experimental study on equal-sized collision of sintered porous ice spheres: Porosity dependence of collisional sticking

SHIMAKI, Yuri^{1*}, ARAKAWA, Masahiko²

¹Environmental Studies, Nagoya University, ²Graduate School of Science, Kobe University

The formation process of planetesimals in protoplanetary disk thought to be involved in collisional process of dust aggregates, but has not been fully understood yet. The relative collision velocity of dust aggregates in protoplanetary reaches several 10s m/s. Recent numerical and experimental studies suggest that the collisional sticking growth of silicate dust aggregates in protoplanetary disk cease at centimeter size because of bouncing barrier [1]. Another numerical simulations about collision of highly porous dust aggregates indicate that icy dust aggregates could grow in size up to ~50 m/s [2], but for icy material it is necessary to consider sintering of ice particles [3]. In this study we performed the low-velocity collisions of isometric porous ice spheres with the porosity from 40% to 80% and examined the effect of sample porosity on the restitution coefficient and the deformed volume by impact.

All experiments were conducted in a large cold room at temperature of -10 °C at Institute of Low Temperature Science, Hokkaido University. The samples were sintered porous ice spheres with a diameter of 30 mm and a porosity of 40% to 80% (mass of 7.52-2.54 g). The ice particles used to construct the samples had an average diameter of ~28 μm and prepared by freezing small water droplets in liquid nitrogen. The ice particles were put into a spherical mold and compressed gradually. To distinguish the projectile from the target, the target was made up by colored ice particles prepared by adding red ink. By using two-stage release system, samples with same porosity were collided during free fall with relative velocity of 0.43-4.12 m/s at nearly head-on. The samples were landed on an airbag. The collisional behavior was recorded by two high-speed video cameras perpendicularly and the impact and rebound velocity (V_i , V_r) and the impact parameter were measured, then the restitution coefficient ($e=V_r/V_i$) was calculated. After the impact experiment, the mass and contact area during impact were measured.

All of the collisional outcomes were classified into bounce, no-bounce and sticking according to the recorded video images. The restitution coefficient of porous ice was found to be independent on the impact parameter and the impact velocity, but strongly dependent on the porosity (P) and become zero at 70% porosity. By comparing our data to result of polycrystalline ice [4], we obtained empirical equation as follows;

$$e=11.3(1-P)^{-0.9\log(1-P)}.$$

The contact area during impact was found to increase with the increase of the impact velocity and the porosity. The relationship between the estimated deformation volume and the impact energy was fitted by power law equation and found that its slope is 0.81 to 1.31, indicating that they are almost proportional. If we assume that the impact kinetic energy was divided into the rebound kinetic energy and volume deformation, the dynamic compressive strength to achieve required deformation was found to be 2-4 times larger than the static compressive strength.

[1] Blum 2010, Res. Astron. Astrophys. 10 1199. [2] Wada et al. 2009, Apj 702 1490. [3] Sirono 1999, A&A 347 720. [4] Higa et al. 1996, Icarus 44 917.

Keywords: Ice, dustaggregate, impact, restitution coefficient, planetary formation

Experimental Studies on Impact Disruption of Rocky Rubble-Pile Bodies

FUJITA, Yukihiro¹, ARAKAWA, Masahiko^{2*}, HASEGAWA, Sunao³, SHIMAKI, Yuri¹

¹Graduate School of Environmental Studies, Nagoya University, ²Graduate School of Science, ³Japan Aerospace Exploration Agency

Rubble-pile bodies, which are constructed from the rocky fragments accumulated gravitationally, are common in the history of the solar system. It is important to evaluate the effect of the rubble-pile structure on the impact disruption in order to clarify the collision process of the solar system bodies. In particular, the impact strength Q_{D*} is an important parameter for planetary collisional evolution. Then, we carried out high velocity impact experiments using several types of rubble-pile targets constructed from glass beads, and we examined the disruption condition of these rubble-pile targets. It is found that a lot of intact beads of rubble-pile targets were ejected very slowly and the enormous impact energy is necessary to shatter all of the beads constructing the rubble-pile targets. We defined the total mass of the small fragments M_{fsum} as a new parameter of impact disruption for rubble-pile targets, and calculated the crater volume for rubble-pile targets using this parameter, the crater volume is defined by the region where the beads are broken catastrophically. We compared them to that formed on for homogeneous basalt targets by using P_i -scaling and found that the crater on rubble-pile targets was larger than that on basalt targets. Furthermore, in order to understand the characteristics of the impact disruption for rubble-pile targets, we estimated the attenuation rate n of the shock pressure decay with the distance by assuming a billiard collision model and we obtained $n=1.6\sim 2.7$ for the power law index of the propagation distance. From these results, we calculated the energy fraction f defined by the kinetic energy of the projectile transferred into the kinetic energy of the intact beads and we estimated the Q_{D*} of rubble-pile bodies from the re-accumulation condition of the dispersed intact constituents.

Keywords: Rubble-pile body, Impact disruption

Measurement of 3D shape distribution of fragments ejected by impact experiments

SHIMADA, Akira^{1*}, TSUCHIYAMA, Akira¹, KADONO, Toshihiko², MICHIKAMI, Tatsuhiro³, ARAKAWA, Masahiko⁴

¹Department of Earth and Space Science, Graduate School of Science Osaka University, ²Osaka University Institute of Laser Engineering, ³Fukushima National College of Technology, ⁴Graduate School of Science, Kobe University

It has been accepted that impact phenomena play a major role throughout the history of the solar system, such as formation and evolution of asteroids and satellites. Regolith on asteroid's surface is also formed by impact of small celestial bodies and cosmic dust onto the surface. Regolith particles on the asteroid Itokawa, which were recovered by the Hayabusa spacecraft, have been examined. In the preliminary examination, surface structures and size and 3D shape distributions of Itokawa particles were elucidated using x-ray microtomography [1], and micro-surface structures of the particles were observed using high-resolution scanning microscopy [2]. Processes on the asteroid surface will be understood comprehensively together with space weathering [3] and implantation of solar wind noble gases [4].

In this study, we performed impact experiments of cratering and recovered impact fragments to compare the results with regolith particles on Itokawa. The experiments were made using a two-stage light gas gun at Kobe University with the impact velocity of 4 km/s. A projectile was a nylon projectile (2.2 mm in diameter and 2.5 mm in length), and two kinds of a target (10 x 10 x 3 cm), marble (compressive strength of 96.9 MPa) and limestone (compressive strength of 53.9 MPa) were used. If we consider regolith formation process, it is reasonable to expect that ejecta with high velocities was easily lost into space while those with low velocities remained on the asteroid's surface as regolith. Therefore, to compare experimental fragments with regolith particles, it is important to recover fragments by considering their ejection velocities. In previous experiments, however, impact fragments were usually collected without separating their velocities except for a few experiments [5,6]. In the present study, we have developed a collection method, where the target was surrounded by Styrofoam boards. In this method, high velocity ejecta were captured into a Styrofoam, while low velocity ejecta fell down on the bottom of a Styrofoam board.

Recovered impact fragments were analyzed by high-resolution x-ray micro-tomography at Osaka University. In previous studies, analysis of fragments has been made using caliper, micrometer, and/or microscope. Therefore, only a limited data have been obtained on the 3D shape distributions. In the present study, 3D shapes of individual fragments were obtained by the x-ray microtomography, and the 3D shape information was successfully obtained from best-fit ellipsoids and compared with Itokawa particle data, which were obtained by similar method.

From the 3D shape information, we calculated size and shape distributions of fragments with the different impact velocities into the two different targets. There is a tendency that high velocity fragments are more spherical than low velocity ones irrespective of the targets. Moreover, low velocity fragments have similar 3D shape distribution to Itokawa particles. This is consistent with the expectation that Itokawa particles should be low velocity fragments ejected by cratering.

[1] Tsuchiyama A. et al. (2011) *Science*, 333, 1125-1128. [2] Matsumoto T. et al., (2012) JGUM abstract, this volume. [3] Noguchi T. et al. (2011) *Science*, 333, 1121-1125. [4] Nagao K. et al. (2011) *Science*, 333, 1128-1131. [5] Asada, N. (1985) *J. Geophys. Res.* 90, 12445-12453. [6] Yamamoto S. and Nakamura A. M. (1997) *Advances Space Res.*, 20, 1581-1584.

Keywords: Impact experiments, Cratering, Regolith, X-ray microtomography

A study on identification of terrestrial impact craters using spectral data obtained by ASTER

YAMAMOTO, Satoru^{1*}, MATSUNAGA, Tsuneo¹, NAKAMURA, Ryosuke², SEKINE, Yasuhito³, HIRATA, Naru⁴

¹NIES, ²AIST, ³Univ. of Tokyo, ⁴Univ. of Aizu

The 182 terrestrial impact craters have been identified so far [1]. This number is much lower than those on the other solid bodies in the Solar System such as Moon, Mars, or Venus. On the Earth, most of structures of impact craters have been eroded and tectonized. In addition, some of preserved impact structures may have been buried or obscured by sediments and vegetation. However, since there are few studies on the global survey of terrestrial impact craters using satellite remote sensing, it is still unclear whether or not more impact craters are preserved on the Earth. The recent survey by Google Earth images discovered a new impact crater in Egypt, which has been already identified as impact origin by the later geophysical analysis [2]. In addition, four new impact structures were confirmed as terrestrial impact craters last year [1], suggesting the existence of more unidentified impact craters on the Earth. Therefore, it is expected that more candidate structures of impact craters would be found by the global survey using satellite remote sensing data.

In this study, we discuss the feasibility to find candidates of impact craters using spectral data by the Advanced Spaceborne Thermal Emission and Reflection Radiometer (ASTER) instrument, which is an imaging instrument with 14 bands, from the visible to the thermal infrared wavelengths, onboard NASA Terra satellite. We show that the discrete concentric patterns in the multispectral data obtained by ASTER can be identified for several terrestrial impact craters. We also analyze the ASTER data for volcanos or dome structures formed by intrusive rocks. Based on these results, we will discuss the feasibility of global survey to identify terrestrial impact craters by ASTER data.

[1] Earth Impact Database, 2012, <http://www.passc.net/EarthImpactDatabase/> Accessed: 02/Feb./2012.

[2] Folco, et al., The Kamil Crater in Egypt. *Science*, 329, pp.804-804, 2010.

Habitable Zone and Water World Regime around Main-Sequence Stars

TAJIKA, Eiichi^{1*}, KADOYA, Shintaro²

¹The University of Tokyo, ²The University of Tokyo

Habitable zone (HZ) around main-sequence stars is defined as an orbital region in which H₂O may exist as liquid water on the surface of terrestrial planets. The inner and outer limits of HZ should correspond to the condition of total evaporation and total freezing of water, respectively. It is, however, assumed implicitly that the atmosphere has enough greenhouse effects due to greenhouse gasses, such as CO₂, CH₄, and NH₃, to maintain the climate warm enough for H₂O to be liquid phase. In this respect, HZ is not a sufficient condition but just a necessary condition for H₂O to be liquid water. That is to say, if there is not enough greenhouse effect, liquid water on the planet should freeze totally even when the planet is orbiting within HZ.

The condition for the planets to have liquid water on the surface is affected not only by semi-major axis (distance from the central star) but also by other factors such as orbital eccentricity, obliquity, degassing rate of CO₂ via volcanism, carbonate-silicate geochemical cycle, land-sea distribution, water abundance, and so on. It is therefore suggested that the concept of HZ should be extended to include these factors.

We also propose a sufficient condition for H₂O to be liquid water if the planet has abundant H₂O on the surface. This is an absolutely habitable zone, and we name it a "Water World Regime" (WWR). It is defined as an orbital condition which permits H₂O as liquid phase unless there is no greenhouse gas other than water vapor in the atmosphere. If there is H₂O on the planetary surface, it is in a liquid phase owing to the energy flux from the central star and greenhouse effect of water vapor without any other greenhouse gasses in the atmosphere. Ice giants and icy satellites around gas giants and/or ice giants, as well as terrestrial planets, are expected to have oceans if they are orbiting within the WWR.

Keywords: Extrasolar planetary system, habitable zone, habitable planet

Debris Disk Ejected by Giant Impacts: Its Dynamical and Chemical Influences on the Terrestrial Planets

GENDA, Hidenori^{1*}, KOKUBO, Eiichiro², SASAKI, Takanori³, UENO, Yuichiro³, IIZUKA, Tsuyoshi¹, IKOMA, Masahiro¹

¹Department of Earth and Planetary Science, The University of Tokyo, ²Division of Theoretical Astronomy, National Astronomical Observatory of Japan, ³Department of Earth and Planetary Sciences, Tokyo Institute of Technology

During the last stage of terrestrial planet formation called the giant impact stage, Mars-sized protoplanets collide with each other. These collisions among protoplanets have a large influence on the various features such as the number of terrestrial planets formed, their mass, and spin state (Kokubo and Genda 2010). Giant impacts are highly energetic events and are responsible for the creation of large satellites, such as the Moon and planets with extremely large cores such as Mercury.

Genda et al. (2012) performed more than 1000 simulations of giant impacts to investigate the merging criteria for giant impacts. We made further analysis of the collision outcomes, and found that significant amount of colliding protoplanets is ejected during giant impacts. In the typical giant impact that occurs during the giant impact stage, several percents of protoplanets are ejected from protoplanets. We developed the hybrid code that includes both orbital evolution of protoplanets and impact process of protoplanets, and investigated the total amount of ejected material during the giant impact stage. We found that about 10% of the mass of the planetary system is ejected. We also found that such ejected materials contain metallic iron. In this study, we focus on the ejected materials by giant impacts, and investigate the dynamical and chemical influences of such ejected materials on the terrestrial planets.

Ejected materials have a dynamical influence on the orbits of the terrestrial planets through the gravitational interaction and reaccretion. Especially, gravitational interaction between ejected materials and terrestrial planets decreases the eccentricity of the terrestrial planets down to the present level (~ 0.01). Using N-body simulation of such configuration, we confirmed that the eccentricity of the terrestrial planets decreases down to 0.01.

Ejected materials also have a chemical influence on the terrestrial planets. Especially, re-accretion of metallic iron would greatly increase the concentration of highly siderophile elements in the Earth's mantle, which would be source of supply of late veneer. Additionally, re-accretion of metallic iron changes redox state of the Earth's surface from oxidized state to reduced state. Reduced surface environment will be maintained for about 1 Gyr.

Keywords: giant impact, BARAMAKI, late veneer, redox state

Newly proposed formation process of terrestrial ocean: Application to the early evolution of Earth and Venus

SASAKI, Takanori^{1*}, GENDA, Hidenori², UENO, Yuichiro¹, IIZUKA, Tsuyoshi², IKOMA, Masahiro²

¹Tokyo Institute of Technology, ²The University of Tokyo

Many possible sources of water on the Earth have been proposed so far (Matsui & Abe, 1986; Gomes et al., 2005; Ikoma & Genda, 2006). Recently, the snow line is considered to pass the heliocentric distance of 1 AU during the planet formation stage (Oka et al., 2011). How much amount of water accumulated into terrestrial planets should be a fundamental question. From the viewpoint of origin and evolution of life, it is also considered to be necessary to accumulate (or escape) of proper amount of water on the early Earth.

There is a paradox of redox state of early Earth. The chemical analysis based on the incorporation of cerium into zircon crystals showed that the mantle reached its present-day oxidation state (FMQ) about 4,350 Myr ago (Trail et al., 2011). On the other hand, the isotopic analysis of sulfur requires the Earth's atmosphere to be maintained reductive at least 2,500 Myr ago (Farquhar et al. 2000). For Venus, there is a problem about the escape of ocean. The hydrogen would escape from the Venus by hydrodynamic escape while the oxygen would be left behind even though thermal/non-thermal escape and oxidation of surface are considered. The oxygen inevitably concentrates in the Venusian atmosphere (Sasaki & Abe, 2008).

In this paper, we propose a new scenario for loss and re-formation of ocean based on Genda et al. (in prep.) as below: (1) Accretion of Fe into primitive ocean as late veneer makes the ocean lose and generates hydrogen atmosphere. (2) Hydrodynamic escape of the hydrogen atmosphere and re-formation of ocean by adding the volcanic gas into the atmosphere occur. (3) One ocean mass is generated taking about one billion years. (4) Coexistence of oxidative mantle and reductive atmosphere on early Earth is realized. (5) Two times ocean loss produces CO₂-dominated Venusian atmosphere.

Our new scenario present an exhaustive framework of early evolution of terrestrial planets especially for the formation of ocean on the Earth. The scenario would be able to applied to extrasolar terrestrial planets as well.

Keywords: formation of ocean, early evolution of planets, Earth, Venus, atmospheric escape, redox

Structure of the proto-atmosphere on Titan accreted in a gas-starved circumplanetary disk

OKADA, Hidetaka¹, KURAMOTO, Kiyoshi^{1*}

¹Department of CosmoSciences, Hokkaido University

Titan, the largest satellite in the Saturn system, is characterized not only by its size comparable to the rocky planets but also by its thick N₂ rich atmosphere with the surface pressure as high as 1.5 bar. Recent Cassini gravity measurements imply that its interior is differentiated into a rock-rich core and ice-rich shell. It is therefore likely that Titan has been gone through melting of ice during its history. To understand the origin of atmosphere and the differentiation of interior, it is important to clarify the thermal evolution and possible atmosphere formation of Titan during accretion.

Supposing gas-free accretion, Kuramoto and Matsui (1994) estimated the thermal evolution of an accreting Titan considering the blanketing effect of a steam atmosphere formed by vaporization of icy component. According to their calculation, the surface temperature exceeds the melting point of H₂O ice thereby Titan differentiates if the accretion time is within 10⁵ yr. Simultaneously, the surface temperature rises above 500 K, which cause significant outflow of atmosphere from Titan's gravity field. However, according to more plausible scenario for the satellite formation, satellites are accreted in gas-starved circumplanetary disks (Canup and Ward, 2002, 2006). This theory implies that Titan captured H₂ and He gas from the gas disk. This study, therefore, estimates the thermal structure of the proto-atmosphere which is in hydrostatic equilibrium with a gas-starved circumplanetary disk and discusses its possible roles in differentiation of Titan and origin of N₂ rich atmosphere.

The proto-atmosphere is assumed to consist of mixture of disk gas component (H₂, He) and volatilized gas component (H₂O) with isothermal stratosphere and troposphere where temperature follows the moist-adiabatic lapse rate under hydrostatic equilibrium with the surrounding disk gas. Hydrostatic structures are solved by changing tropopause. By solving the radiation transfer equation regarding H₂ and H₂O as continuum absorptions, we calculated the outgoing thermal radiation from the top of atmosphere for each hydrostatic structure. The disk temperature and pressure at the orbit of Titan is estimated by a disk model (Canup and Ward, 2002)

For the atmosphere in hydrostatic equilibrium and continuously connected with the surrounding disk, there exists the upper limit of the surface temperature about 300 K. If the surface temperature is higher than upper limit, the assumption of hydrostatic equilibrium and continuousness breaks up and the outflow of proto-atmosphere is likely induced because the pressure at the Hill radius becomes higher than the disk pressure.

By comparing outgoing thermal radiation from the top of the atmosphere with the accretional energy flux, one can estimate that the surface temperature exceeds the melting point of H₂O during accretion if the accretion time is shorter than 10⁶ yr. Moreover, there exists the upper limit of thermal radiation for the hydrostatic atmospheres. This is about 400 W/m², which is equal to the accretional energy flux when the accretion time is 0.4 Myr. Since Titan likely accreted within 10⁴ yr to 10⁶ yr, the surface temperature may exceed the critical temperature due to the heating by the difference in accretional energy and thermal radiation during accretion. In this case, the outflow of proto-atmosphere is expected to occur.

When such outflow occurs, it is likely that H₂, He, and rare gases insoluble to water escape preferentially. The building blocks of Titan likely contain NH₃ as a icy component. Because NH₃ is highly soluble into water, NH₃ likely remains on the satellite surface even if outflow occurs. Chemical conversion of remaining NH₃ to N₂ may explain why the present atmosphere of Titan is N₂ rich but Ar poor in spite of their similarities in chemical properties and cosmic abundance. Impact induced shock chemistry is a candidate mechanism to produce N₂ from NH₃ on the proto-Titan (McKay et al., 1988).

Numerical modeling of hydrodynamic escape from early Earth atmosphere

UMEMOTO, Takafumi¹, KURAMOTO, Kiyoshi^{1*}

¹Department of CosmoSciences, Graduate School of Sciences, Hokkaido University

The anoxic early Earth's atmosphere is considered to change its composition from some reduced one to oxidative one associated with hydrogen escape to space. Its changing rate is a clue for discussing whether the early Earth's surface environment is better suited for synthesizing organic compounds or not and for understanding climate changes on early Earth. In previous studies, escape of hydrogen was believed to occur rapidly by hydrodynamic escape driven by strong EUV radiation from the young Sun. Recently, Tian et al. (2005, hereafter T05) investigated numerically the hydrodynamic escape of hydrogen from the atmosphere of early Earth and indicated that the escape rate was lower than previously thought and thereby reduced surface environment might be maintained for long periods. However, the calculation of T05 has a critical problem that the conservation of mass is not satisfied.

In this study, we first performed recalculations of T05 and tested the accuracy of calculation for hydrodynamic escape with the Lax-Friedrichs scheme which they adopted. As a result, we found that their calculation does not satisfy the mass conservation owing to the strong numerical diffusion and the calculated escape rate increases with decreasing contribution of numerical diffusion by changing the configuration of numerical grids. We therefore conclude that T05 underestimates the hydrodynamic escape rate.

We then constructed a new numerical model of the one-dimensional time-dependent nonviscous hydrodynamic equations for a single constituent atmosphere in spherical geometry with CIP & CIP-CSL2 method and performed the calculation with same parameter as T05. As a result, our new model predicts hydrodynamic escape rates are 5-10 times larger than those of T05 when the number density at the bottom is larger than $n_0 = 5 \times 10^{18} \text{ m}^{-3}$ and the solar EUV flux is larger than 2.5 times than that of today. However, decreasing the energy deposition rate to atmosphere, the hydrodynamic escape rates of this study becomes smaller than those of T05. This is because the energy loss by heat conduction from upper boundary, which is taken to be zero in T05, becomes significant under such conditions.

Using our new results, we may estimate the hydrogen mixing ratio of about 7% for the anoxic atmosphere in the late Archean by balancing the geologically estimated volcanic hydrogen outgassing rate with hydrodynamic escape rate under the solar EUV 2.5 times that of today. In addition, the hydrogen mixing ratio had been rising through Archean because of the decrease in solar EUV flux. The increase in hydrogen mixing ratio might result in CO₂-poor atmosphere, which would destabilize climate system. This result might be consistent with the occurrence of snowball earth event at 2.2 Gyr ago.

Keywords: Hydrodynamic escape

Two evolutionary paths of early terrestrial planets with steam atmospheres

HAMANO, Keiko^{1*}, ABE, Yutaka¹, GENDA, Hidenori¹

¹The University of Tokyo

Recent studies with N-body simulations suggest that Earth-sized planets would experience giant impacts among planetary-sized bodies during formation, implying that the planets would form in a globally molten state. Orbital crossing during the giant impact stage would cause significant radial mixing of material throughout the terrestrial planet formation region. It means that even the planets located close to their host star would still have a chance to acquire some water during formation.

Our goal is to clarify controlling processes of thermal history and water budget of terrestrial planets after the last giant impact until the magma ocean solidifies. Since water vapor is a potent greenhouse gas, the amount of steam atmosphere would strongly affect the thermal history of the planets. On the other hand, high solubility of water into silicate melts suggests that the amount of steam atmosphere would be controlled by water exchange between the atmosphere and the magma ocean. Elkins-Tanton (2008) calculated atmospheric growth and solidification time of the magma ocean, considering such a water exchange. In her model, the effect of condensation of water is neglected on outgoing planetary radiation. Also, it is assumed that the total amount of water of the planets is constant during solidification.

As reported by Nakajima et al. (1992), however, water-saturated atmospheres have radiation limits. The values of the radiation limits are common to the planets with the same mass, while the planet closer to the host star receives the larger incident stellar flux. Therefore, the existence of the radiation limits could make a fundamental difference in the cooling rates of the planets located at different orbital distance from their star. The recent studies with N-body simulations also suggests that planet formation lasts about 10-100 Myr. Strong EUV radiation from a young host stars could drive intense hydrodynamic escape of atomic hydrogen, which would also affect the amount of steam atmosphere and therefore the cooling rate of the planets.

We developed a steam-atmosphere and magma-ocean coupled model, in which a radiative-convective equilibrium model of grey atmosphere was incorporated in order to consider the effect of condensation of water vapor on planetary radiation. Water loss caused by the hydrodynamic escape was also taken into account. Using this model, we investigated solidification time and water budget of Earth-like terrestrial planets orbiting around a Sun-like star with respect to planetary orbital radius and initial water inventory.

Our results suggest that there would be two types of evolutionary paths of terrestrial planets, depending on orbital radius. The condition that separates the two distinctive evolutionary paths is whether the net incident stellar flux that the planet receives exceeds the value of the radiation limit from steam atmosphere or not. In this presentation, we will show the controlling mechanisms and also its implications to exoplanet observations and the early evolution of Earth and Venus.

Keywords: Magma ocean, Giant impact, Thermal history, Water budget, Hydrodynamic escape, Radiation limit

Estimation of Cooling Rate for H₂-He Atmosphere with Radiative Convective Equilibrium Model

TAKAHASHI, Yasuto^{1*}, ISHIWATARI, Masaki¹, KURAMOTO, Kiyoshi¹

¹Hokkaido University

In planetary atmosphere, it is generally thought that vertical convection is one of the major power sources of any atmospheric circulations. Intensity of these convections is dependent on atmospheric cooling rate, and atmospheric thermal structure is maintained by the equilibrium of this cooling and heating by convection carrying energy from lower hot atmosphere. This mechanism can be also occurred in the case of Gas Giant Planets, such as Jupiter, which have a thick atmosphere mainly consisted of hydrogen molecules.

In our study, we computed the radiative features and tried to reveal how they are determined, with calculation of energy transportation by radiation and convection in H₂-He atmosphere. We assumed plane parallel atmosphere, and calculated radiative transfer with formulations based on Appleby and Hogan (1984) in range 0.002-2 bar supposing the present Jovian atmosphere. The atmosphere consists of H₂ and He, and we took into account the collision induced absorptions of these molecules (Borysow 1988, 2002) as opacity sources. We calculated radiative transfer for each 10 cm⁻¹ bin over range 10-990 cm⁻¹. The solar radiation is neglected. At lower boundary, temperature was fixed and the flux from lower atmosphere was given by diffusion approximation. After the calculation of radiative transfer, we determined if the convective instability occurs at each layer, and gave dry adiabatic temperature profile for the entire unstable layers. We repeated these sequences until the time variation of thermal structure becomes small enough. Then, we got the energy equilibrium thermal structure.

In our results, the calculated vertical profile of cooling rate is almost consistent with the previous study by Sromovsky et al. (1998) base on the data of Galileo probe. The profile has a peak at 0.7 bar. At this level, optical depth for all wavenumber becomes nearly 1, so emission can effectively go through outward to space. This is the reason why such a profile is maintained. The peak value of cooling rate is 0.016 K/day, and which is much smaller than the typical value of the Earth's tropopause. This is due to the much lower temperature of the Jovian atmosphere. We also found that cooling rate approaches zero toward lower boundary. This might mean that the lower boundary of troposphere exists around 2 bar.

Keywords: gas giant planet, atmosphere, cooling rate, radiation, convection

Vertical wavenumber spectra of gravity waves in the Venus atmosphere

ANDO, Hiroki^{1*}, IMAMURA, Takeshi²

¹University of Tokyo, ²ISAS/JAXA

Vertical wavenumber spectra of Venus gravity waves were obtained for the altitude range 65-80 km from temperature profiles acquired by the Venus Express radio occultation experiments and classified in terms of four latitude regions; equatorial region (0-20 degree), middle latitude region (20-50 degree), high latitude region (50-80 degree), polar region (80-90 degree). As a result, the spectra, which cover vertical wavelengths from 1.5 to 15 km, generally show a decline of the spectral density with wavenumber similarly to those obtained in the terrestrial stratosphere and mesosphere. Moreover we compared observed spectrum with the theoretical spectrum of the saturated gravity waves described as Tsuda et al. (1991) and Tsuda and Hocke (2002). In equatorial region, spectral density is lower than those in the other latitude regions by up to one order of magnitude and does not reach the saturation value. This implies that gravity waves are not saturated in the equatorial region. In middle latitude region, logarithmic slope of the spectrum is nearly -4, although its density is near the saturation value. In high latitude and polar region, spectral density is almost consistent with theoretical saturation spectrum, which suggests that gravity wave saturation occurs also in these regions in the Venus atmosphere.

Moreover we calculated the intensity scintillation spectra near the altitude of 70 km from the time development data of the received intensity and classified in terms of four latitude regions as described above. As a result, spectral densities in the high latitude and polar region are 3-4 times as large as in the equatorial and middle latitude regions and Kolmogorov inertial subrange could be seen. This implies that turbulent diffusion associated with the gravity wave breaking occurs in these regions.

Keywords: Venus atmosphere, Gravity wave, Vertical wavenumber

Current status of Subaru Strategic Exploration of Exoplanets and Disks (SEEDS)

KUSAKABE, Nobuhiko^{1*}, TAMURA, Motohide¹, KANDORI, Ryo¹, Tomoyuki Kudo¹, Jun Hashimoto¹, SEEDS/HiCIAO/AO188 team²

¹National Astronomical Observatory of Japan (NAOJ), ²Project team

From the space- and ground-based survey for exoplanets, the number of planets are going to exceed 3,000, including candidates. These discoveries lead us to a variety of planets which are called hot-Jupiter, hot-Neptune and super-Earth. However, our understanding of planetary systems and their formation is far from complete. A census of companions to stars over a wide range of ages will provide important clues to the formation and evolution of stars, brown dwarfs, and planets.

SEEDS is the first Subaru Strategic Observations to conduct the high contrast camera HiCIAO with 188 elements Adaptive Optics (AO188) imaging survey searching for giant planets as well as protoplanetary/debris disks at a few to a few tens of AU regions around ~500 nearby solar-type or more massive young stars. The ages of our exoplanet target stars span ~1-10 Myr for YSOs in nearest star forming regions, through ~100-500 Myr old stars in nearby open clusters, to ~1 Gyr old nearby stars. The protoplanetary disk targets are the YSOs in nearby star forming regions, while the debris disk candidates include both well known and newly discovered ones from Spitzer/AKARI satellites.

As demonstrated with one of recent successes of direct imaging of proto-planetary disks, we revealed the geometry of the disk of young (~10Myr) YSO, AB Aur. The disk structure shows the rich features and most inner part of the disk. Another recent success is the imaging for HR 4796 A their debris ring. The ring features imply existence of unknown inner planets. Previous observations show simple disks but HiCIAO+AO188 revealed their complex disk structures which imply inner unknown planets. These results lead us to be connecting the planet formation research field and proto-planetary research field, which fields went on apart previously.

SEEDS project observations are from September 2009 to 5 years. The interesting results are increasing, in the first half of our project time. In this talk, I would like to present about the middle status report not only disks but also direct detection of planet mass objects.

Keywords: Exoplanet, Proto-planetary disk, Near infrared, Direct imaging

Surface Density Distributions of Protoplanetary Disks with Dead Zones of Magneto-Hydrodynamic Turbulence

TAKEUCHI, Taku^{1*}, OKUZUMI, Satoshi², MUTO, Takayuki¹

¹Tokyo Institute of Technology, ²Nagoya Univeristy

We study evolution of the surface density distributions of protoplanetary disks taking into account the effect of turbulent viscosity via magneto-rotational instability. The inner part of a protoplanetary disk is inactive to MHD turbulence because of its low ionization degree. In such a region, called as a dead zone, gas accretion due to turbulent viscosity is suppressed, and consequently the gas from the outer part accumulates, making the surface density of the inner part higher than that of the outer part. At the outer boundary of the dead zone, which locates from a few AU to several tens AU, the surface density of the disk is expected to have a jump. Such surface density structures are expected to be detected by future dust continuum observations of ALMA.

The radial extent of the dead zone is determined by the ion-electron recombination on the dust surfaces, and depends of the total surface area of the dust particles. As the dust particles grow, the dead zone shrinks radially. There is an accretion flow at the surface of the dead zone, and its accretion rate depends on the strength of the vertical magnetic fields. The jump in the surface density depends on the vertical magnetic fields. Because the vertical magnetic fields advect or diffuse with the gas, both the gas density profile and the vertical magnetic fields should be determined self-consistently.

In this study, as a first step, we consider the case where the plasma beta is constant with radius. The ionization degree of the gas is calculated for various values of the dust particle size and the gas accretion rate, and then the extent of the dead zone and the surface density structure of the disk are determined. The ionization degree and accretion rate are calculated using the approximated formulae of Okuzumi (2009, ApJ, 698, 1122) and Okuzumi & Hirose (2011, ApJ, 742, 65), respectively. For the accretion rate of $10^{(-8)}$ M_{sun} / yr, the dust size of 1 micron, and the vertical magnetic fields of 0.1 mG, the surface density jumps 3 times at 20AU, and for stronger magnetic fields, the jump becomes weaker. For larger dust particles, the dead zone shrinks. We also discuss the effect of advection and diffusion of the vertical magnetic fields on the surface density structure of the disks.

Keywords: planet formation, protoplanetary disks, magnetohydrodynamic turbulence

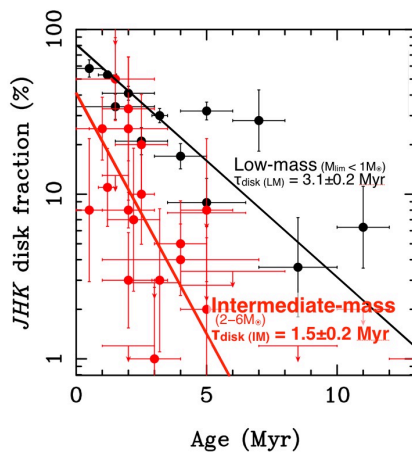
The Lifetime of Protoplanetary Disks Surrounding Intermediate-mass Stars

YASUI, Chikako^{1*}, Naoto Kobayashi¹, SAITO, Masao², Alan T. Tokunaga³

¹University of Tokyo, ²National Observatory of Japan, ³IfA, University of Hawaii

To quantitatively and comprehensively study the lifetime of protoplanetary disks surrounding intermediate-mass stars (~2-6 solar mass), we derived their disk fraction (IMDF) only using near-infrared JHK photometric data with a robust method with which the IMDF can be derived with high accuracy. We applied this method to all well-known nearby (heliocentric distance of $< \sim 3$ kpc) and young ($< \sim 5$ Myr) clusters. The derived JHK IMDFs appear to approximately follow an exponential decay with the cluster age. From the best fit of the decay curve, the characteristic decay timescale for intermediate-mass stars is found to be 1.5 plus or minus 0.2 Myr with an initial IMDF of 42 plus or minus 11 %. The estimated decay timescale is about half of that for low-mass stars (about 3 Myr), showing the decay timescale is proportional to $M_{*}^{-0.5}$ plus or minus 0.2, where M_{*} is stellar mass. This is consistent with previous works that qualitatively suggest this dependence. As for the disk lifetime, which is defined as the timescale of disk fraction to bottom out, we found that the outer MIR-disk traced by *Spitzer* 8 μ m excess have about 4 Myr longer lifetime than K-disk, which is the innermost dust disk traced by K-band excess emission. Because such time-lag is not seen for low-mass stars, this long “transient phase” may be a special characteristics for intermediate-mass stars, such as higher planet formation rate for higher mass stars, and faster inner disk dispersal compared to low-mass stars.

Keywords: protoplanetary disk, disk evolution, intermediate-mass stars, exoplanet



Rapid formation of Saturn after Jupiter completion

KOBAYASHI, Hiroshi^{3*}, Chris Ormel², IDA, Shigeru¹

¹Department of Earth and Planetary Science, Graduate School of Science and Technology, Tokyo Institut, ²Astronomy Department, University of California, Barkeley, ³Department of Physics, Nagoya University

Although planets can rapidly migrate through the interaction with massive gas, Jupiter stays at the current location probably without significant migration. Jupiter is thus expected to have finished its formation during the depletion of gas nebula. Therefore, the following formation of Saturn should have occurred in a short timescale, about several million years. Since the core of Saturn is estimated to be about 10 Earth masses, it would be formed via core accretion. Although planetesimal accretion produces a core, a massive core induces the fragmentation of planetesimals, resulting fragments are then removed by their radial drift due to gas drag, and eventually the growth of the core stalls because of the reduction of surrounding bodies. After the completion of Jupiter formation, Jupiter formed a gap in the solar nebula. Since the drift velocities of fragments are lower around pressure maximum produced just beyond the gap in the nebula, the core of Saturn grows rapidly through the accretion of such fragments. At first, we investigate the case of no radial drift around the pressure maximum. In the minimum-mass solar nebula (MMSN), kilometer sized planetesimals can produce a core exceeding 10 Earth masses in several million years. Larger planetesimals need larger amount of solid, 3 times MMSN for 10 km and 10 times MMSN for 100 km. However, fragments drift due to their eccentric and inclined orbits even in the pressure maximum region. Fragments can halt inside the pressure maximum and may contribute the growth of the core. If we assume that such fragments cannot accrete onto the core, the depletion of fragments then stalls core growth. In MMSN, a core resulting from kilometer-sized planetesimals grows rapidly but the core reach only 2 Earth masses due to the depletion of fragments. Despite severe setup, a core can exceed 10 Earth masses within about one million years from kilometer-sized planetesimals in a disk with solid surface density larger than 4 times MMSN. Since the core can reach the critical core mass even in the severe case, Saturn would have formed in such a disk via core accretion.

Keywords: Planetary formation, Collisional fragmentation, Saturn

Gas Accretion Flow onto Circumplanetary Disks from Protoplanetary Disks: Effect of Gap

TANIGAWA, Takayuki^{1*}, Masahiro N. Machida², OHTSUKI, Keiji³

¹CPS / ILTS, Hokkaido University, ²Faculty of Sciences, Kyushu University, ³Faculty of Sciences, Kobe University / CPS

Satellite systems around gas giant planets are thought to be formed in circum-planetary disks, which are believed to exist at the gas capturing growing phase of giant planets. However, the structure of the circum-planetary disks are poorly known and thus current formation theories of satellite systems are forced to be constructed under not-well-established disk structures, which could impact the results.

In this study, we performed a series of hydrodynamic simulations of gas accretion flow onto circum-planetary disks from proto-planetary disks in order to analyze the structure of circum-planetary disks. In order to obtain fine structure of the gas flow around the planet, we employ nested grid method, which enable us to calculate high-resolution structure with high efficiency. In our previous studies, we do not consider the effect of gap, which would be created by the gravity of giant planets. But, this time, we consider the effect of gap to see if the accretion flow structure changes.

We found that, when there is a gap with symmetry about planetary orbit, the power-law distribution function of gas accretion flux onto the disk, which we obtained in the previous work, does not change almost at all. However, when the gap has some asymmetry, the distribution function of the accretion flow becomes more center-concentrated. This result under the more realistic setting would be important for the formation and evolution of the circumplanetary disks, which produce satellite systems.

Keywords: Satellite formation, giant planets, hydrodynamics

Development of an anelastic convection model in rotating spherical shells for stars, gas and icy giant planets.

SASAKI, Youhei^{1*}, TAKEHIRO, Shin-ichi², NAKAJIMA, Kensuke³, KURAMOTO, Kiyoshi⁴, HAYASHI, Yoshi-Yuki⁵

¹Dept. Math., Kyoto Univ., Kyoto, Japan, ²RIMS, Kyoto Univ., Kyoto, Japan, ³Dept. Earth Planet. Sci., Kyushu Univ., Fukuoka, Japan, ⁴Dept. CosmoScience, Hokkaido Univ., Sapporo, Japan, ⁵CPS/Dept. Earth Planet. Sci, Kobe Univ., Kobe, Japan

The problem of convection in rotating spherical shells has been studied vigorously as a fundamental model of global convection presumably emerging in celestial bodies, such as stars, gas and icy giant planets, and terrestrial planetary interiors. Recently, according to development of numerical computational abilities, fundamental aspects and characteristics of convection has been revealed and knowledge about this issue is increased under the assumption of Boussinesq approximation, which ignores compressibility of the fluid. However, characteristics of compressible convection in rotating spherical shells has not been understood yet compared with Boussinesq convection, although some studies performed so far use the anelastic approximation in order to deal with compressibility. Compressibility is an important element for discussing deep convection of stars and gas and icy planets, since thickness of their convection layers is several times larger than the scale height. Not only for these celestial bodies but also for extra-solar gas giant planets, which have been discovered with recent sophisticated technologies of astronomical observation, compressibility cannot be ignored for considering fluid motion in their interiors. Investigation of effects of compressibility on convection in rotating spherical shells would contribute to the basic knowledge of fluid motions in the interiors of these many celestial bodies.

Based on the consideration described above, we are now developing a numerical model of an anelastic fluid in rotating spherical shells in order to assess effects of compressibility on convective motions. On the development of the model, we extended our numerical model of Boussinesq convection in rotating spherical shells developed so far to the anelastic system. We described mass flux with poloidal and toroidal potentials instead of velocity field in the case of Boussinesq fluid. This procedure enables us to extend our Boussinesq model constructed so far to the anelastic case in a natural way.

In the presentation, results of some numerical experiments using our newly developed model will be shown, and future plan is also discussed.

Keywords: Convection in rotating spherical shells, Compressible convection, Anelastic equations

Revisited to the impact erosion of early Earth atmosphere during the heavy bombardment period

KUROSAWA, Kosuke^{1*}, HAMANO, Keiko², SUGITA, Seiji³, KADONO, Toshihiko⁴

¹ISAS, JAXA, ²Graduate School of Science, The Univ. of Tokyo, ³Graduate School of Frontier Science, The Univ. of Tokyo, ⁴Inst. of Laser Eng., Osaka Univ.

Impact-induced expanding vapor clouds resulting from hypervelocity impacts accelerate the surrounding planetary atmosphere. If the velocity of an accelerated atmosphere exceeds the escape velocity of the planet, the atmosphere is lost from the planet. This process is called impact erosion, which has been widely studied since 1980s. Especially, the early dense atmosphere of Mars ($\sim 10^5$ Pa) was lost due to impact erosion during the heavy bombardment period [Melosh & Vickery, 1989].

In this study, we focused on the impact erosion of early Earth atmosphere during heavy bombardment. Melosh & Vickery (1989) roughly estimated the required impact velocity for the massive blow off of the atmosphere above the tangent plane on the Earth as ~ 25 km/s. In contrast, the median of impact velocity of asteroids onto the Earth is considered as 13-15 km/s [Chyba, 1991]. Thus, the impact erosion of Earth atmosphere has not been studied well. However, they employed the minimum value of the internal energy of the expanding vapor cloud for a conservative estimate because energy partitioning during hypervelocity impacts at higher than the escape velocity of the Earth was highly uncertain. Now, the Hugoniot curve up to ~ 1 TPa are available obtained using high power lasers. The equation for the internal energy of an expanding vapor cloud is modified using the pressure-entropy Hugoniot curve from the conservative estimate and is incorporated into the sector blow-off model, which is a semi-analytical model for impact erosion due to expanding vapor clouds [Vickery & Melosh, 1990]. We found that the threshold impact velocity for the initiation of atmospheric blow-off estimated by our equation is ~ 13 km/s, which is ~ 3 km/s smaller than that estimated by the conservative estimate of the internal energy. The significance of the impact erosion of the early Earth atmosphere may be drastically changed from the current understanding because the median of impact velocity between the Earth and asteroids is located between the threshold velocities between both estimates.

In presentation, we are planning to present the systematic results on the change in the total atmospheric pressure as functions of impact velocity, initial atmospheric pressure, the total mass of impactor, the size distribution of impactor and to discuss the atmospheric evolution of the Earth during the heavy bombardment period.

Keywords: Impact-induced vapor clouds, Early Earth atmosphere, Impact erosion, Heavy bombardment period, Solar nebula, Noble gases

Differentiation of silicates from H₂O ice in an icy body induced by ripening

SIRONO, Sin-iti^{1*}

¹Graduate School of Environmental Sciences, Nagoya University

Planetary differentiation is the process of the separation of the constituents of a planetary object as a consequence of their physical and chemical behavior. Distinct layers are developed in the object, and the denser materials sink to the center while the lighter materials rise to the surface.

One of the probable scenarios of differentiation between silicate-ice in an icy object is the settling of a silicate particle in water after melting of the object. In order for settling to proceed or occur, the size of a particle should be sufficiently large such that the settling velocity of the particle must exceed the background flow velocity induced by thermal convection. The sizes of the particles change because of dissolution and precipitation. This process is called ripening. In this study, I derive the critical particle sizes required for settling and the timescales for growth of the particles to these sizes through ripening. It is observed that settling is possible if the silicate particles coagulate with each other to form a network in water. If the particles do not coagulate, the probability of the occurrence of settling is low because the time duration required for the particle growth to the critical size is large. The coagulation of silicate particles strongly depends on the pH of water.

Keywords: Icy body, Differentiation, Ripening, Composition

Hypersonic wind tunnel experiments on chemical reaction around an icy object with ablation using electric discharge

SUZUKI, Kojiro^{1*}, WATANABE Yasumasa²

¹GSFS, The University of Tokyo, ²Grad. Sch. Eng., The University of Tokyo

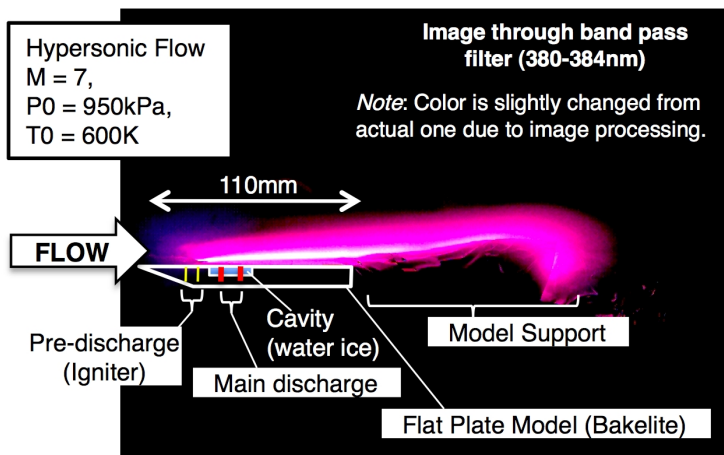
When an extraterrestrial object enters the planetary atmosphere, a strong shock wave is formed in front of the object, and various gaseous materials including prebiotic ones are produced in the high temperature shock layer flow by the chemical reactions of the atmospheric gas and the ablation gas injected at the surface. Such products are distributed into the atmosphere through the wake flow behind the entry object. We conducted the numerical analyses of the Navier-Stokes equations for the chemically reacting hypersonic flow around an icy object with the ablation injection of H₂O in the N₂-CO₂ atmosphere (Suzuki, AIAA Paper 2011-3756, 2011). The nonequilibrium chemistry of the 28 species (N₂, O₂, N, O, NO, NO⁺, e⁻, N⁺, O⁺, N₂⁺, O₂⁺, C, C₂, C₃, CO₂, CO, CN, CO⁺, C⁺, H, H₂, HCN, HCO, C₂H₂, C₂H, CH, H₂O, OH) is considered as well as the thermal nonequilibrium described by the two-temperature (translational and vibrational) model. The computational results show that HCN is produced near the surface in the stagnation region by the chemical reaction of H₂, which comes from the decomposition of the ablation gas, and CN, which is produced behind the shock wave in front of the object. HCN is transported into the atmosphere via rapid expansion flow at the shoulder and the wake flow in almost frozen state. In the case of an icy sphere of 0.2 m radius with the uniform ablation rate 0.05 kg/(s m²) over the windward surface at the flight velocity, altitude and atmospheric composition 8 km/s, 60 km (equivalent to the present earth) and CO₂:N₂=0.93:0.07, respectively, the mass flux of HCN exhausted into the wake flow is in the order of 0.01% relative to the total mass loss rate of H₂O.

The hypersonic wind tunnel facility, which is used in the aerospace engineering for research and development of a re-entry vehicle for the space transportation, is also a powerful tool to simulate the high-speed flow around an extraterrestrial entry object and the various phenomena caused by the ablation (Suzuki, et al., JpGU Meeting 2010, PPS004-10, 2011, PPS020-22, Imamura et al., AIAA Paper 2010-4512). Due to the operation limit of the facility, however, it is impossible to make the flow temperature high enough to excite the chemical reactions. Then the thermal energy was added to the flow by the electric discharge at the electrodes put on the surface of the test piece (Watanabe and Suzuki, AIAA Paper 2011-3736). The experiments were conducted at the hypersonic and high-enthalpy wind tunnel of the graduate school of frontier sciences, the University of Tokyo (http://daedalus.k.u-tokyo.ac.jp/wt/wt_index.htm). The figure shows a picture taken at a trial experiment using a flat plate model. In addition to the electrodes, a cavity having ice inside was installed on the plate. The ablation occurred at the surface of the cavity in the hypersonic flow. The image was taken through the narrow band pass filter at 380-384nm, where the emission of CN is observed. The stagnation temperature and the pressure on the surface are about 600K and 300Pa, respectively. The quasi-steady electric discharge was kept for about 1 sec at 5V and 6A. At the center of the discharge region, the vibrational temperature is estimated as about 6000K by the spectroscopy and the fitting technique for N₂(1+) band. The high luminous region indicates the presence of CN, which is produced from N in the air and C in the ablation gas of the Bakelite, from which the plate is made.

As seen in the above, the hypersonic wind tunnel experiment using the electric discharge seems promising for simulating the chemical reactions around the atmospheric entry object with ablation.

This work is supported by Grant-in-Aid for Scientific Research (B) No. 21360413 of Japan Society for the Promotion of Science.

Keywords: atmospheric entry, hypersonic flow, wind tunnel, ablation, ice, chemical reaction



The Condition Dividing Aqua Planets and Land Planets: Effects of Water Amount on Planetary Climate

WAKIDA, Miyuki¹, TAKAO, Yuya¹, GENDA, Hidenori^{1*}, ABE, Yutaka¹, O'ISHI, Ryouta², ABE-OUCHI, Ayako³

¹Department of Earth and Planetary Science, The University of Tokyo, ²Atmosphere and Ocean Research Institute, The University of Tokyo, ³Center for Climate System Research, The University of Tokyo

Liquid water on the planetary surface is essential for habitability of the planet. There are two processes that determine water distribution on a planet: the transportation on the planetary surface, which depends on its topography, and the transportation through atmospheric circulation. A planet whose water distribution is controlled by the former transportation is called 'an aqua planet', and the planetary surface is always wet (Kasting, et al. 1993). A planet whose water distribution is controlled by the latter transportation is called 'a land planet' (Abe et al. 2005).

Since a planet with very small amount of water should have the characteristics of a land planet, Abe et al. (2011) performed numerical experiments with general circulation model (GCM) for such planets. They found that liquid water localizes in high latitudes and dry desert appears in low latitudes. They also found that the habitable zones of land planets are much wider than that of aqua planets. Thus, it is important to investigate the condition dividing aqua planets and land planets.

Abuku (2009) considered that a globally linked ocean is required for being an aqua planet. Using mathematical percolation theory, he found that the ocean is globally linked when the ocean covers about 50% of the planetary surface. He concluded that the dividing condition is 50% of the ocean coverage.

However, it is not clear that a globally linked ocean is really the dividing condition. Although lowland area becomes ocean in percolation theory, on a land planet liquid water localizes in high latitudes, which means that lowland area is not always ocean. Therefore we should perform GCM experiments for a planet with topography, and check his result. In this study, we made four kinds of random topography maps and systematically performed numerical experiments with the transportation of liquid water on the surface with various amount of water.

We found that the condition dividing aqua planets and land planets is not sharp, which has not been shown in Abuku (2009). The change from land planet to aqua planet gradually occurs as water content increases. We can classify the climate state into three types: land-planet state, aqua-planet state and the marginal state. We also found that the coverage rate of the ocean rather than water content is essential for that classification. The climate of the planet is like land planet for 0.3 of ocean coverage, aqua planet for more than 0.5 and marginal state for 0.3-0.5.

Keywords: habitable zone, land planet, aqua planet, GCM

The habitability of terrestrial planet that is covered with ice but has an internal ocean

UETA, Shoji^{1*}, SASAKI, Takanori¹

¹Tokyo Institute of Technology

Recently, extrasolar (bound) terrestrial planets and free-floating (unbound) planets have been discovered. It is important theme whether habitable bound and unbound terrestrial planets exist. On the other hand, snowball planets those are covered with ice shell are thought to have internal ocean melting by geothermal heat flow from the interior. The habitability of the internal ocean has been discussed in many papers. In this paper, for different values of the planetary mass, the distance from the central star, the water abundance, and the abundance of radiogenic heat sources, we discuss the conditions for bound and unbound terrestrial planets to have an internal ocean for the timescale of planetary evolution owing to geothermal heat flux from the planetary interior. We show that a planet with 1 Earth's mass without greenhouse gas can have an internal ocean if it has 0.5-8 times Earth's water abundance or more than 0.4 times Earth's abundance of radiogenic heat sources at 1 AU. If it has more than 8 times Earth's water abundance, high-pressure ice produced at the bottom of the ocean would make the internal ocean uninhabitable. The condition for a planet to have an internal ocean strongly depends on the planetary mass. It is easier to have the internal ocean if the planet is super-Earth. A free-floating planet with 1 Earth's mass without greenhouse gas can have an internal ocean if it has 2-8 times Earth's water abundance or more than 2 times Earth's abundance of radiogenic heat sources. It could be uninhabitable if it has more than 8 times Earth's water abundance. In the extrasolar and free-floating planets, terrestrial planets with internal ocean are more common than Earth-like "ocean planets." So, we should consider not only "ocean planets" but also "snowball planets" with internal ocean.

Keywords: exoplanets, terrestrial planets, habitability, internal ocean, radiogenic heat, free-floating planets

A Study on the Water World Regime around Extrasolar Planetary Systems and Planetary Environments

FUKUSHIMA, Satoshi^{1*}, KADOYA, Shintaro¹, TAJIKA, Eiichi²

¹Department of Earth and Planetary Science, The University of Tokyo, ²Department of Complexity Science and Engineering, The University of Tokyo

Habitable zone (HZ) is defined as an orbital range around a main sequence star where planets could have liquid water on the surface (e.g., Kasting et al., 1993). It is, however, noted that, liquid water cannot exist on the surface of a planet without sufficient greenhouse effects of the atmosphere due to some greenhouse gasses, such as CO₂ and CH₄, even if the planet is orbiting within HZ (Tajika, 2008). In this sense, HZ is not a sufficient condition but just a necessary condition for the planets with liquid water.

There should be, however, an orbital condition for the planets which are close enough to their central stars to warm the climate to have liquid water without any other greenhouse gasses except water vapor in the atmospheres (Tajika, 2008). Such a condition is named here 'Water World Regime' (WWR).

In this study, the condition for WWR is estimated using a one dimensional (1-D) energy balance climate model with a radiation model for steam atmosphere. The 1-D radiative-convective equilibrium model of Nakajima et al. (1992) is adopted for outgoing infrared flux from the planet.

The orbital range of WWR is found to be approximated by an annual mean insolation from 243.4 to 293.9 W/m². When the central star is the sun and orbital eccentricity is 0, the inner and outer boundaries correspond to 0.84 AU and to 0.94 AU, respectively. This range is very narrow compared with the traditional HZ (0.84 to >1.37 AU). This is because WWR is defined here as the condition for the planets without greenhouse gas in the atmosphere except for water vapor in contrast to the traditional HZ which implicitly assumes strong greenhouse effects of the atmosphere. Among the extrasolar planets discovered so far, there are 12 candidates for the planets which satisfy the WWR condition.

Keywords: extrasolar planet

Evolution of terrestrial planets with water loss

KODAMA, Takanori^{1*}, GENDA, Hidenori¹, ABE, Yutaka¹, Zahnle, Kevin²

¹The University of Tokyo, ²NASA Ames Research Center

Liquid water on the planetary surface is thought to be important for the origin and evolution of life. The region from the central star where liquid water is stable in the planetary surface has been called the habitable zone (HZ). Kasting et al. (1993) [1] estimated the width of the HZ around various types of the main sequence stars for Earth-like planets (called aqua planet). The width of the HZ is located between 90% and 110% of the incident solar radiation that the present Earth receives.

Abe et al. (2011) [2] considered a hypothetical planet with very small amount of water (called land planet). On a land planet, the water circulation is limited in the atmospheric circulation. The distribution of ground water is determined by the local balance between precipitation and evaporation. Using the general circulation model (GCM), they estimated the inner and outer edges of the HZ. They found that the width of the HZ for a land planet is located between 77% and 170% of the incident solar radiation that the present Earth receives. This result means that the width of the HZ for land planets wider than that for aqua planets. They proposed a new planetary evolution pathway on their study. It is the evolution from the aqua planet to the land planet by water loss. However, this planetary evolution pathway has not been discussed in detail.

These two studies indicated that the amount of water on the planetary surface is important to habitability of the planet. We focus on the evolution of water content on the planet by considering the water loss and discuss the evolution from the aqua planet to the land planet.

Using numerical model, we calculate the evolution of water content on the planetary surface and discuss the evolution from the aqua planet to the land planet. We use the hydrodynamic escape model [3,4] as a water loss mechanism considering the time-dependent stellar evolution [5,6,7] and treat the initial amount of water, the distance from the central star, the mass of the central star and the mass of the planet as a parameter to offer suggestion to observations of extrasolar terrestrial planets.

There are two important timescales for the evolution from the aqua planet to the land planet. One is the timescale of loss of ocean by water loss and another is the timescale of increasing of radiations from the central star. If the former is shorter than the later, the aqua planet evolves to the land planet. When the aqua planet with the Earth mass around the star like Sun and its orbital radius is 0.75 [AU], the boundary of the initial amount of water is 0.15-ocean mass (1 ocean mass is the present ocean mass of Earth). The aqua planet evolves to the land planet if the initial amount of water is less than this boundary.

Extrasolar planets that have been observed have various masses and orbit around various types of stars. In general, stars with low mass relative to the Sun are dim and the evolution of them is slow. Planets with a mass higher than Earth have a strong gravity relative to Earth. It is mean that super-earths around stars with low mass hard to evolve from the aqua planet to the land planet. However, the habitable duration of a planet that evolved to the land planet is longer than that of a planet that was considered on the classical HZ. This result means that the number of sample of habitable extrasolar planet by observations increases.

Reference

- [1] Kasting, J. F., Whitmire D. P., and Reynolds, R. T. (1993). *Icarus*, 101, 108-128.
[2] Abe, Y., Abe-Ouchi, A., Sleep, N. H., and Zahnle, K. J., (2011). *Astrobiology*, 11, 443-460. [3] Guinan, E.F., Ribas, I., 2002. Vol. 269. *Astron.Soc. Pacific,SanFrancisco*, pp.85-106. [4] Walker (1977) [5] Gough, D. O (1981) *Solar Physics*, vol. 74, Nov. 1981, p. 21-34 [6] Iben, I. (1967) [7] Lammer et al. (2009). *A&A*, 506, 399-410.

Keywords: terrestrial planet, habitable zone, extrasolar planet

Variety in atmospheric compositions of terrestrial exoplanets: effects of surface H₂O mass

HONG, Peng^{1*}, SEKINE, Yasuhito¹, SUGITA, Seiji¹

¹Complexity Sci. & Eng., Univ. of Tokyo

Theoretical models predict that a significant part of Earth-sized to super-Earth-sized terrestrial exoplanets possess a deep surface H₂O ocean (e.g., > 100 km depth), given accretion of H₂O-rich planetesimals (e.g., carbonaceous chondrites and comets). The atmospheric compositions of these exoplanets also may have a wide variety depending on the surface H₂O mass, because the redox state of degassing volatiles from the mantle is significantly influenced by the depth of ocean. According to studies of Earth's volcanoes (Holland, 2002), the chemical compositions of gas species degassed from subaerial volcanoes are generally oxidizing, while those from submarine volcanoes are more reducing. The difference between the compositions of volcanic gas species reflects the difference of the thermodynamic conditions of the magmas (Kump & Barley, 2007). Here, we investigate the variety of atmospheric compositions of terrestrial exoplanets by focusing on surface H₂O mass. We discuss the possibility of presence of reducing atmospheres on exoplanets with deep surface oceans.

To investigate CH₄/CO₂ ratios in degassing volatiles from mantle as a function of ocean depth, we adopted thermodynamic equilibrium between CH₄ and CO₂ in a hydrothermal fluid. We assumed that the equilibrium is determined by the hydrogen fugacity, controlled by mineral redox buffers. Terrestrial subaerial volcanic gases are considered to equilibrate with fayalite-magnetite-quartz (FMQ) buffer (Holland, 2002). Measured oxidation states of deep-sea hydrothermal systems are close to the pyrrhotite-pyrite-magnetite (PPM) buffer (McCollom & Seewald, 2007). By assuming that the rock components of terrestrial exoplanets are similar to those of Earth, we used the FMQ and PPM buffers to calculate the hydrogen fugacity and consequent CH₄/CO₂ ratios of gas species from hydrothermal systems on these planets.

We investigated the atmospheric compositions for a given flux and composition of gas species degassed from mantle, developing a one dimensional photochemical model based on an early-Earth model (Pavlov et al., 2001). Our model contains 337 reactions and 69 species involved in H, C, N, O, and S chemistry. Calculations were carried at 1 bar and 275 K of surface condition. The model also includes UV shielding effect by organic haze using an experimental relation between C/O ratio and produced aerosol mass (Trainer et al., 2006). The partial pressure of CO₂, *p*CO₂, is considered to be controlled by chemical weathering rate in the carbon cycle. We varied *p*CO₂ from 0.1 to 1000 times the present atmospheric level, because of the large uncertainty in chemical weathering rate on exoplanets.

The thermodynamic calculations show that the redox state of outgassing fluids become significantly reducing under high-pressure conditions (> 7000 bar). Even if the rock components of exoplanets are similar to that of Earth, CH₄ would be predominant in carbon-bearing species degassing from mantle when the surface oceans are deeper than 70 km.

Our photochemical calculations indicate that exoplanets with deep surface oceans would have reducing atmospheres (CH₄/CO₂ ratio > 1), when the degassing fluxes reach a level several times that of Earth. Considering the variations in Earth's CO₂ degassing flux in the past (Tajika & Matsui, 1993), exoplanets with deep surface ocean are capable of possessing a Titan-like, hazy atmosphere, which could be detectable by future observations. The photochemical model also shows that the CH₄ mixing ratios reach high levels (i.e., 10 - 1000 ppm) at the degassing fluxes comparable to that of current Earth. These results suggest that radiative forcing of CH₄ should be taken into account when considering surface temperature and habitability of exoplanets with deep surface oceans.

Keywords: exoplanets, hydrothermal system, photochemistry, atmospheric composition

Surface environment of water-rich extraterrestrial planets with carbon cycle under various obliquities and geographies

WATANABE, Yoshiyasu^{1*}, TAJIKA, Eiichi², KADOYA, Shintaro¹

¹Earth and Planet. Sci., Univ. of Tokyo, ²Complexity Sci. & Eng., Univ. of Tokyo

Water-rich terrestrial planets like the Earth are expected to be found in the extrasolar planetary systems in the near future. To discuss habitability of planets, we have to investigate characteristic features of climate system of the water-rich terrestrial planets. One of the key factors which controls climate is "obliquity", that is, the inclination of planet's axis. Considering a large influence of obliquity on the solar energy distribution on the planetary surface, obliquity variations could induce large climate change on the planets. The climate of the Earth has been stabilized on long timescales by a negative feedback mechanism involving removal of CO₂ from the atmosphere by weathering of silicate minerals on land followed by carbonate precipitation in oceans, and continuous supply of CO₂ from the planetary interiors to the atmosphere via volcanism. This mechanism should be required for water-rich extraterrestrial planets to maintain warm climate stably. Without this mechanism, the climate of planets cannot be stabilized against changes in the various climate forcings. Considering that the amount of weathering is strongly influenced by surface temperature and the area of continent available for weathering, and that temperature of continent responds to the insolation more rapidly than that of oceans, long-term climate mode would be different under different obliquity or geography.

While the climate of extraterrestrial planets with high obliquities was investigated by Williams and Kasting (1997), there are few studies which systematically investigate the effects of obliquity change on the climate of the planets with carbonate-silicate geochemical cycle. In this study, we therefore investigate systematically the climate of the water-rich terrestrial planets with a negative feedback mechanism of carbonate-silicate geochemical cycle under various obliquities, semi-major axes and different geographies.

We tested with 3 different geographies; "Slice" (continent is distributed at the same fraction for each latitude.), "Equatorial" (supercontinent is centered around the equator.) and "Bipolar" (supercontinent is centered around both poles.). We found that, while the "permanent ice-cap mode" (partially ice-covered throughout the year) and the "seasonal ice-cap mode" (partially ice-covered seasonally) exist stably at low obliquities, the ranges of semi-major axis for these climate modes shrink and finally disappear with an increase of obliquity. This is because latitudinal gradient of annual mean insolation becomes smaller with an increase of obliquity, resulting in meridional heat transport to be insufficient. When carbonate-silicate geochemical cycle is taken into account, the ranges of semi-major axis for all the climate modes expand at any obliquities, compared with the cases without carbon cycle, indicating that the carbon cycle strongly stabilizes the climate for the planets with any obliquities inside the habitable zone. These features are found at any geographies. Dependence of obliquity on climate modes is quite different among different geographies. The climate is cold for lower obliquities at Equatorial geographies, whereas the climate is cold for higher obliquities at Bipolar geographies. This characteristic of climate modes at Slice geography is intermediate, but is closer to those of Equatorial characteristic. The results derive from a negative feedback of carbonate-silicate geochemical cycle. If continent is centered on the equator, at the same semi-major axis, pCO₂ decrease with the decrease of obliquity, because weathering occurs effectively throughout 1 year at lower latitude where annual mean insolation and land fraction are large. In contrast, if continent is centered on poles, pCO₂ decreases with the increase of obliquity at the same semi-major axis, because weathering occurs effectively throughout 1 year at higher latitude where seasonal insolation largely changes and land is the largest.

Keywords: obliquity, carbonate-silicate geochemical cycle, continental distribution, exoplanet, habitability, planetary climate

Long-term Evolution of Surface Environment on Extrasolar Planets with Carbonate-Silicate Geochemical Cycle

KADOYA, Shintaro^{1*}, TAJIKA, Eiichi², WATANABE, Yoshiyasu¹

¹Earth and Planetary Sci., Univ. of Tokyo, ²Complexity Sci. & Eng., Univ. of Tokyo

Surface environment of extrasolar terrestrial planets has been discussed in terms of presence of liquid water. Kasting et al. (1993), for example, estimated habitable zone (HZ) in which the planets are able to have liquid water on its surface. They found that the inner and outer limits of HZ are 0.95 and 1.37 AU, respectively. They also considered the change of HZ due to stellar evolution, and suggested that HZ moves outward and diminishes with time. In their study, sufficient amount of greenhouse gas is assumed, but it has not been verified quantitatively.

We investigate the conditions where planets hold liquid water, considering their surface temperature and the amount of greenhouse gas. Surface temperature is estimated with one-dimensional energy balance model (North et al. 1981; Williams & Kasting, 1997; etc.). The greenhouse gas is assumed to be CO₂, and its amount in the atmosphere is controlled by carbonate-silicate geochemical cycle, in which degassing rate is given and chemical weathering rate depends on surface temperature and partial pressure of CO₂.

The results show that, with the degassing rate as much as that at present Earth's value, planets can avoid snowball mode until 1.05 AU from the central star. This limit may be much narrower than the one estimated from previous studies. However, if the degassing rate of CO₂ is higher, the outer limit moves outward farther from the central star. Under such condition, a planet has higher partial pressure of CO₂, which makes meridional temperature distribution much uniform, resulting in shrink of partial ice cap.

The degassing rate of CO₂ becomes lower with time. In order to examine such effect, we consider thermal evolution of the planet (Tajika & Matsui, 1992) and consider on the long-term stability of surface climate.

Keywords: extrasolar planet, carbonate-silicate geochemical cycle, EBM

The Complete Evaporation Limit for Land Planets: A Study with 1D EBM

TAKAO, Yuya^{1*}, Hideori Genda¹, Takanori Kodama¹, Yutaka Abe¹

¹Department of Earth and Planetary Science, the University of Tokyo

Liquid water is thought to be essential for the origin and evolution of life on the Earth. Planets globally covered with liquid water just like the Earth are called 'aqua planets'. Using 1D radiative-convective model, Nakajima et al. (1992) discussed the presence of the critical flux of planetary radiation that an aqua planet can emit. If the atmosphere is saturated with water vapor, there appears an upper limit (critical flux) on infrared radiation the planet can emit. If net insolation exceeds the value, an aqua planet cannot emit energy that balances with incoming solar radiation. Then the surface temperature increases until the troposphere comes unsaturated, thus there no longer exists liquid water on its surface. According to their analytic model, the critical flux is about 123 % of net insolation of present Earth.

On the other hand, there could be planets that have liquid water not globally but locally. Abe et al. (2005) investigated the climate of a theoretical planet with very small amount of water using 3D general circulation model (GCM). They showed that the local balance between precipitation and evaporation of water makes liquid water localize in high latitudes, and low latitudes become dry desert. Such a planet is called a 'land planet'. According to their numerical experiments, liquid water on a land planet is completely evaporated when net insolation exceeds 170 % of present Earth (for an Earth-sized planet with 1 bar atmosphere). We call such limit the 'complete evaporation limit'.

The complete evaporation limit was investigated for a certain limited condition of a planet (1 bar air atmosphere, 0 obliquity and no transport of ground water). Our goal is to understand the mechanisms that determine the complete evaporation limit. For the first step, we investigate the dependence of the complete evaporation limit on the transport of ground water, which affects the localization of the ground water. We modified the 1D gray model used by Nakajima et al. (1992) in order to consider the partly unsaturated atmosphere of land planets. We use a meridional 1D energy balance model (EBM) used by North et al. (1981). The transport of ground water and water vapor depending on mass gradient are also taken into account. We carried out numerical experiments with various efficiencies of the transport of ground water.

We found that if ground water exists from the pole to low latitudes, the complete evaporation limit is the same value as the critical flux for aqua planets; therefore the climate is similar to that of aqua planets. As ground water becomes localized, the complete evaporation limit gradually gets larger. Thus, the complete evaporation limit is controlled by the degree of ground water localization. The extent of ground water is controlled by the balance between the transport of ground water and water vapor in the atmosphere. These results imply that even if the atmospheric composition or pressure changes, we can estimate the extent of ground water as long as we know the transport of water vapor and ground water; consequently we can estimate the complete evaporation limit, if we know the relationship between complete evaporation limit and the extent of ground water.

In addition, in order to understand the mechanism of complete evaporation, we carried out an analysis on the stability of the surface temperature using a very simple model, in which the planet is divided into two regions, the dry region and wet one, and energy is transported beyond the boundary. As a result, at insolation slightly smaller than the complete evaporation limit, the wet high latitudes emit planetary radiation at a little smaller rate than the critical flux of aqua planets. It implies that complete evaporation occurs even if the wet region is not required to emit radiation exceeding the critical flux.

A balloon borne telescope for planetary observations

YAMAMOTO, Mutsumi^{1*}, TAGUCHI, Makoto¹, Kazuya Yoshida², SAKAMOTO, Yuji², Toshihiko Nakano², Yasuhiro Syoji³, TAKAHASHI, Yukihiro⁴

¹Department of Science, Rikkyo University, ²Department of engineering, Tohoku University, ³Japan Aerospace Exploration Agency, ⁴Department of Science, Hokkaido University

In order to study various time-dependent phenomena in planetary atmospheres and plasmas, continuous observation is important. However, machine time of ground-based large telescopes is limited and good seeing and good weather are not necessary guaranteed during observation time slot. We have been developing a balloon-borne telescope for planetary observations from the polar stratosphere where a planet can be observed continuously.

In this system, a Schmidt-Cassegrain telescope with a 300-mm clear aperture is mounted on a gondola whose attitude is controlled by control moment gyros, an active decoupling motor, and attitude sensors. The gondola can float in the stratosphere for periods longer than 1 week. Pointing stability of $0.1''$ rms will be achieved by the cooperative operation of the following three-stage pointing devices: a gondola-attitude control system, two axis telescope gimbals for coarse guiding, and a tip/tilt mirror mount for guiding error correction.

The first experiment of the balloon-borne telescope system was conducted on June 3, 2009 at Taikicho, Hokkaido targeting Venus. However, the balloon experiment failed due to trouble with an onboard computer. The balloon borne telescope was re-designed for the second experiment in August in 2012, when the target planet is Venus.

Keywords: Balloon, Telescope, Atmosphere, Planet, Venus, Stratosphere

A repository for knowledge of planetary science serving by Center for Planetary Science (CPS)

SUGIYAMA, Ko-ichiro^{1*}, SUZUKI, Ayako¹, Tomoaki Nakamura², Sho MANABE², SAKAI, Shotaro³, Ryoichi Tsurumaki³, Shimpei Tatsumi², NAKAOKA, Reina², Noriyuki Katoh², Iori Tani², UMEMOTO, Takafumi³, OSHIKAWA, Tomomi³, Center for Planetary Science¹

¹Center for Planetary Science, ²Graduate school of Science, Kobe University, ³Department of CosmoSciences, Graduate School of Science, Hokkaido University

We provide a repository for knowledge of planetary science, in other words, a digital library of lectures as one of the services for planetary science communities at CPS (Center for Planetary Science). We record lectures in seminars and workshops and publish the lecture video and presentation files on the Internet. The repository gives an opportunity for a participant's review and a non-participant's study and contribute to the inter-university and international education. The accumulation of knowledge and findings encourage activity overlooking origin, revolution and diversity of planetary systems as a whole.

In order to promote the service, we arrange equipments and establish work procedure for recording and publication of seminars and workshops, and development of an on-demand system have been performed. By having arranged the work procedure and the on-demand system, the lectures of the CPS seminar which is held once every week are published within the day. Other seminars and workshops sponsored or cosponsored by CPS are also published using the on-demand system. More than 1100 lectures recorded in 11 years from 2001 with presentation files are opened to the public, and these lectures can be searched with a lecturer, a title, etc.

In the presentation, we introduce the repository for knowledge of planetary science and explain the features of the repository.

Reference: <https://www.cps-jp.org/~mosir/pub/>

Keywords: A repository for knowledge of planetary science

Growth and porosity evolution of dust aggregates in protoplanetary disks: Effects on the disk opacity

OKUZUMI, Satoshi^{1*}, TANAKA, Hidekazu²

¹Nagoya University, ²Hokkaido University

Porosity evolution of dust aggregates plays a decisive role in their collisional growth in protoplanetary disks. In this presentation, we show how the evolution of aggregate porosities affects the appearance of the disks at millimeter wavelengths on the basis of our recent numerical simulations of aggregates' growth and porosity evolution. We find that our new porous aggregate model predicts a monotonic decrease in the opacity index beta toward the central stars, in marked contrast to previous compact aggregate models predicting the emergence of the peak of beta at several tens of AU. This difference allows us to test the porosity models by millimeter observations of protoplanetary disks.

Keywords: dust, coagulation, porosity, opacity, protoplanetary disk

Binary formation in Planetesimal Disks

DAISAKA, Junko^{1*}, KOKUBO, Eiichiro¹

¹National Observatory of Japan

As of April 2010, 48 TNO (trans-Neptunian Object) binaries have been found. This is about 6% of known TNOs. However, in previous theoretical studies of planetary formation in the TNO region, the effect of binary formation has been neglected. TNO binaries can be formed through a variety of mechanisms, such as three-body process, dynamical friction on two massive bodies, inelastic collisions between two bodies etc. Most of these mechanisms become more effective as the distance from the Sun increases. In this paper, we studied three-body process using direct N-body simulations.

We found that, Chaos-Assisted-Capture (CAC) is the dominant channel of binary formation.

We systematically changed the distance from the Sun, the number density of planetesimals, and the radius of the planetesimals and studied the effect of the binaries on the collision rate of planetesimals. In the TNO region, binaries are involved in 1/3 - 1/2 of collisions, and the collision rate increases by a factor of a few compared to the theoretical estimate for the direct two-body collisions. Thus, it is possible that the binaries significantly enhance the collision rate

and reduce the growth timescale. In the terrestrial planet region, binaries are less important, because the ratio between the Hill radius and physical size of the planetesimals is relatively small. Although the time scale of our simulations is short, they clearly demonstrated that the accretion process in the TNO region is quite different from that in the terrestrial planet region.

We also performed N-body simulations of planetesimal disks from 30 AU - 30.2 AU with planetesimal mass distributions.

We show the formation of binary in trans-Neptunian region is not rare quantitatively.

Disks with high surface density and low random velocity are likely to form binaries easily. There is a tendency of formation of binaries with similar mass components.

Binary formation is almost proportional to the surface density of the planetesimal disk, and almost inversely proportional to the initial random velocity.

Inclination and eccentricity distribution is consistent with the observational result.

Keywords: planetesimal binary, TNO, accretion

Effects of H₂ Dissociation and Recombination on Planetesimal Bow Shocks

YAMAZAKI, Fumika^{1*}, NAKAMOTO, Taishi¹

¹Department of Earth and Planetary Sciences, Tokyo Institute of Technology

Chondrules are mm-sized particles included in many meteorites. There are evidences that they have experienced heating and melting, but the details of the heating event are still unknown. One of the ideas for heating mechanism is the shock wave heating model. The model explains that, when the precursor dust grains run into the shock, they experience the gas drag heating, and dust temperature exceeds the melting point. Based on this idea, Ciesla et al. (2004) and Nakajima et al. (2012, in preparation) conducted numerical simulations of planetesimal bow shocks and examined them as a chondrule formation site. They assumed that the gas consists of hydrogen molecules and the gas changes adiabatically; the effects of H₂ dissociation and recombination were ignored. However, the calculated temperature behind the shock front was 4000K or more (Nakajima et al. 2012, in preparation), so H₂ dissociation is expected to occur. Once the dissociation of H₂ takes place, the resultant temperature of the gas would be different. Thus, to understand bow shocks around planetesimals, the gas flow should be investigated with H₂ dissociation/recombination.

We conduct numerical hydrodynamics simulation with H₂ dissociation and recombination around planetesimals. We develop an equilibrium calculation code of H₂ dissociation/recombination and add it to the ZEUS-2D code.

Our simulation results show that the gas temperature is lower and the density is higher in front of planetesimals than the results by adiabatic calculations. This can be understood as a result of the H₂ dissociation. Moreover, in the region where the recombination occurs, the temperature is higher than the one of adiabatic calculation. Also the positions and the figurations of the shock fronts are slightly different between both calculation results.

These results suggest that the H₂ dissociation and recombination may affect the heating of chondrule precursors. That is because the gas drag heating is susceptible to the gas density. So, the thermal history of dust particles under the effect of H₂ dissociation/recombination should be investigated in the future.

Keywords: bowshock, numerical hydrodynamics simulation, H₂ dissociation, chondrule

Temporary capture of planetesimals by a giant planet

SUETSUGU, Ryo^{1*}, OHTSUKI, Keiji²

¹Dept. Earth Planet. Sci., Kobe Univ., ²Dept. Earth Planet. Sci., Kobe Univ./CPS

Gravitational interaction between planets and planetesimals plays an important role not only in planet formation but also in the origin and dynamical evolution of small bodies in the Solar System. When planetesimals encounter with a planet, in most cases they experience either gravitational scattering by the planet or collision onto it. However, in some cases planetesimals can be captured by the planet's gravity and orbit about the planet for an extended period of time, before they escape from the vicinity of the planet. This phenomenon is called temporary capture, and may have played an important role in the origin of irregular satellites and Kuiper-belt binaries, as well as dynamical evolution of short-period comets.

Recently, we investigated temporary capture of planetesimals initially on eccentric orbits, and found that temporary capture orbits can be classified into four types (Suetsugu et al. 2011). Their orbital size and direction of revolution around the planet change depending on planetesimals' initial eccentricity and energy. When initial eccentricity is so small that Kepler shear dominates relative velocity between planetesimals and the planet, temporary capture typically occurs in the retrograde direction in the vicinity of the planet's Hill sphere, while large retrograde capture orbits outside the Hill sphere are predominant for large eccentricities. Long prograde capture occurs in a very narrow range of eccentricity and energy of planetesimals. We obtained rates of temporary capture of planetesimals and found that the rate of long capture increases with increasing eccentricity at low and high eccentricity but in intermediate values of eccentricity decreases with increasing eccentricity.

In the above study, we performed three-body orbital integrations under Hill's approximations, where the masses of the planet and planetesimals are assumed to be much smaller than the solar mass. In this case, the effect of the curvature of their guiding-center orbits are neglected.

This assumption is valid for the case of low mass planets, but the effect of curvature may be important for temporary capture by a high mass planet, like Jupiter. Previous global orbital integration that investigated temporary capture focused on long-term evolution of small bodies under the influence of multiple giant planets (Kary & Dones 1996).

In the present work, we use a simple three-body system that consists of the Sun, a planet, and a test particle, and perform global orbital integration to examine effects of a high mass planet on temporary capture. We will discuss the characteristics of temporary capture obtained by our global calculation and compare them with our previous results of local three-body calculation.

Keywords: planets, satellites

Capture of planetesimals by circumplanetary disks

FUJITA, Tetsuya^{1*}, OHTSUKI, Keiji², TANIGAWA, Takayuki³

¹Dept. Earth Planet. Sci., Kobe Univ., ²Dept. Earth Planet. Sci., Kobe Univ./CPS, ³Low Temp. Sci. Inst., Hokkaido Univ./CPS

Giant planets capture gas and solid particles from protoplanetary disk by their gravity, and circumplanetary disks are formed around them. The regular satellites of the giant planets (e.g. Galilean satellites) have nearly circular and coplanar prograde orbits, and are thought to have formed by accretion of solid particles in the circumplanetary disk. Because a significant amount of gas and solids are likely to be supplied to growing giant planets through the circumplanetary disk, the amount of solid material in circumplanetary disks is important not only for satellite formation but also for the growth and the origin of the heavy element content of giant planets. Solid particles smaller than meter-scale are strongly coupled with the gas flow from the protoplanetary disk and delivered into the disk with the gas. On the other hand, trajectories of large planetesimals are decoupled from the gas. When these large planetesimals approach a growing giant planet, their orbits can be perturbed by gas drag from the circumplanetary disk depending on their size and random velocity, and some of them would be captured by the disk. In the present work, we examine orbital evolution of planetesimals approaching a growing giant planet with a circumplanetary disk, and evaluate the capture probability.

We deal with the three-body problem for the sun, a planet, and a planetesimal, and assume that the planet has a circumplanetary gas disk. The radial distribution of the gas density is assumed to be given by a power-law, and its vertical structure is assumed to be isothermal. Gas elements in the disk are assumed to rotate in circular orbits around the planet, with an angular velocity slightly lower than Keplerian velocity due to its radial pressure gradient. We turn on gas drag only within the planet's Hill sphere. We integrate Hill's equation including the gas drag term with various initial orbital elements. We consider the following two types of capture: (i) when planetesimals hit the planet, regardless of whether they lose enough energy to become gravitationally bound, (ii) when planetesimals lose enough energy through gas drag and become gravitationally bound within the planet's Hill sphere. Here, we mainly focus on the capture in the case of (ii).

Energy of planetesimals decreases by gas drag when they pass through the disk. Energy dissipation in the case of prograde trajectories (i.e. trajectories in the same direction as the circular motion of the gas) are different from that of retrograde trajectories because the relative velocity between planetesimals and the gas in the case of retrograde trajectories is larger than that of the prograde case. When planetesimals move in the mid-plane of the circumplanetary disk, energy dissipation of each case during one encounter with the planet can be obtained analytically. We find that they agree well with results of orbital integration. In the case of inclined orbits relative to the mid-plane of the disk, energy dissipation is more complicated because planetesimals' trajectories pass through the disk in various ways. When the energy of a planetesimal becomes less than zero within the planet's Hill sphere, it is regarded as becoming captured by the circumplanetary disk. We define the effective capture radius R_c by the distance from the planet at which the energy dissipation equals to the initial energy of a planetesimal. We obtained an analytic expression for R_c and capture probabilities of planetesimals with given initial orbital elements in the coplanar case. We will discuss results of orbital integration for capture rates, including the cases of inclined orbits of planetesimals.

Keywords: circumplanetary disk, gas drag, satellite

The Effect of Magnetic Turbulence on the Formation and Evolution of Circumplanetary Disks

FUJII, Yuri^{1*}, OKUZUMI, Satoshi¹, TANIGAWA, Takayuki², Inutsuka Shu-ichiro¹

¹Nagoya University, ²Center for Planetary Science

We investigate the importance of magnetic turbulence in the evolution of circumplanetary disks. Satellites with almost circular orbits nearly on the equatorial planes of the central planet are called regular satellites. Circumplanetary disks are supposed to be the formation sites of regular satellites. In order to understand satellites formation, we have to understand the evolution of circumplanetary disks. However, the mechanism of gas accretion in circumplanetary disks are poorly known, and thus, the gas accretion rate and the surface density of circumplanetary disks are very uncertain. The most promising mechanism of gas accretion is the magnetorotational instability (MRI), but the size of MRI-active region depends on the density structure of the disk. To understand the overall evolution of circumplanetary disks, we have to analyze the early formation phase of the disk where the matter is continuously provided by the infall from protoplanetary disks. In this work, we calculate the surface density evolution of the disk by solving the alpha-model equation of accretion disk with this infall onto the disk, and we calculate the ionization degree with the method we have developed in Fujii et al. (2011) and estimate the activity of MRI in circumplanetary disks. We find that MRI is not active in most of the phases of the evolution of circumplanetary disks.

Keywords: circumplanetary disks, magnetic turbulence, satellite formation

MERGING CRITERIA FOR GIANT IMPACTS OF PROTOPLANETS : Dependence of Their Composition and Size

FUJITA, Tomoaki^{1*}, GENDA, Hidenori¹, ABE, Yutaka¹

¹Department of Earth and Planetary Science, Graduate School of Science, The University of Tokyo

At the final stage of terrestrial planet formation, collisions between Mars-sized protoplanets, called giant impact, occur frequently. Giant impacts have a large influence on the number and sizes of planets, the formation of the Moon and the large metal core of the Mercury, and so on (Kokubo and Genda 2010). Therefore, the investigation of impact phenomena of giant impacts is important for understanding the characters and early evolution of terrestrial planets in our solar system. These days many extrasolar planets have been discovered around other fixed stars. Recently, the planets with several times the mass of the Earth called super-Earths and the planets almost composed of H₂O have also been discovered. During formation of these planets, it is also considered that collisions between planetary sized objects occur frequently (Ogihara and Ida 2009).

According to Genda et al. (2012), they focused on the giant impacts of protoplanets during terrestrial planet formation in our solar system, and investigated the merging criteria for collisions between protoplanets with the mass from Mars to Earth size composed of rocky mantle and iron core. As a result, they found that about a half of giant impact events that occurred during the giant impact stage was not merging events.

However, the merging criteria obtained by Genda et al. (2012) are not simply applied to the formation of extrasolar planets such as super-Earths and icy planets. In this study, we performed simulations of collisions between super-Earths and icy planets under various impact parameters. We investigated the merging criteria and compared our results with Genda et al. (2012).

We used Smoothed Particle Hydrodynamics method and performed several hundreds simulations under the various impact conditions such as the impact velocity, the impact angle, and the sizes and compositions of planets. As the composition and size of planets, we considered ice, rock, and iron materials, and the sizes with 0-10 times Earth mass.

As a result, in the case of the collision between two Mars-sized planets with icy mantle and rocky core, we found that the merging criteria were the same as the results of Genda et al. (2012). Similarly, in the case of the collision between two Mars-sized planets composed only of icy material and two Mars-sized planets composed only of rocky material, the results were the same. Hence, the merging criteria for giant impacts do not depend on composition of colliding planets if the planetary size is smaller than the Earth.

Additionally, we performed simulations of the collision between two planets with different composition, for example an icy planet and a rocky planet. In this case, we found that the merging criteria changed from that of Genda et al. (2012). Critical impact velocity is lower than the results of Genda et al. (2012). By observing the impact simulation, we noticed that the planet with higher density went through the other, which probably made merging of the two planets difficult.

In the case of the collision between two super-Earths with rocky mantle and iron core, we found that almost head-on collision with high impact velocity tended to be not merging although the other cases were similar to the previous work. As the reason why the results were different from that of Genda et al. (2012), the vaporization of rock is considered. In the case of the collision between super-Earths, a large amount of rocky material vaporizes, which prevents two planets from merging.

References

- Genda, H., Kokubo, E., and Ida, S., Merging Criteria for Giant Impacts of Protoplanets, *ApJ* 744, 137, 2012.
Kokubo, E., and Genda, H., Formation of Terrestrial Planets from Protoplanets Under a Realistic Accretion Condition, *ApJ* 714, L21-L25, 2010.
Ogihara, M., Ida, S., N-Body Simulations of Planetary Accretion Around M Dwarf Stars, *ApJ* 699, 824-838, 2009.

Keywords: giant impacts, extrasolar planets, merging criteria, protoplanets

Planetary migration in accretion disks and formation of Earth-sized planets

YAMADA, Kou^{1*}, Satoshi Inaba²

¹Center for Protoplanetary Science, Kobe University, ²School of International Liberal Studies, Waseda University

Protoplanets form in a disk surrounding a young star. A low-mass protoplanet interacts with a gas disk gravitationally, which leads to a decrease in its semi-major axis. This is called the Type I migration of a planet. It is believed that the Type I migration is one of the most important physical processes in planetary formation. It is caused by the torques acting on a protoplanet by a disk. Recently, it was shown that a protoplanet is possibly trapped in a disk. Hasegawa & Pudritz(2011, MNRAS) comprehensively examined various mechanisms to halt the planet migration in a disk. They showed that a protoplanet might be trapped at the ice line, inside of which all the ice is evaporated and solid particles are composed of rocks and metals. The different opacity laws are used inside and outside of the ice line, resulting in a steep and shallow temperature distributions in the inner and outer regions, respectively. The large corotation torque acting on a protoplanet due to the steep temperature distribution suppresses the negative Lindblad torque in an inner region. On the other hand, the corotation torque on a protoplanet is too weak to cancel the negative Lindblad torque in an outer region. A protoplanet inside and outside of the ice line moves toward the ice line and is expected to accumulate at the ice line. However, it was shown that density waves can be altered by a thermal structure of a disk (e.g., Yamada & Inaba, 2011, MNRAS). It is not clear if protoplanets accumulate at the ice line even when we include dissipation processes in a disk. We make global two-dimensional hydrodynamic simulations and systematically examine the total torque acting on a protoplanet by an optically thick accretion disk, taking dissipation processes in a disk into account.

We study the type I migration of a protoplanet in disks with various opacities. We find that the total torque acting on a protoplanet by a disk strongly depends on opacity of the disk. We adopt a realistic opacity model and find that the sign of the total torque could change around the ice line of a disk. It is found that the total torque becomes zero in the region inside of the ice line if the timescale for the viscosity is nearly equivalent to the turnover time in the horseshoe orbit. This means that the accretion rate of the disk needs to be smaller than 2×10^{-8} solar mass/yr for the protoplanet to move outward in the optically thick accretion disk. Furthermore, using the N-body simulations, we investigate whether the accumulation of protoplanets around the ice line can accelerate further growth of protoplanets or not.

Keywords: planetary system, planetary migration, terrestrial planet, type I migration, density wave

Change in fayalites with ultraviolet rays and water

KOMORI, Nobuo^{1*}

¹Minamirokugo junior high school

I have been doing an experimental research of weathering on rocks by ultraviolet rays and waters in a junior high school science club since 2002. This time, it aimed to see the reaction of fayalite when it is soaked in distilled water and irradiated with ultraviolet rays.

It is said that there is much basalt that perhaps contains fayalite on Mars' surface. Moreover, it is estimated that there was water in Mars' surface in the past. Therefore, I think that ultraviolet rays and water are one of the factors which change rocks on Mars' surface.

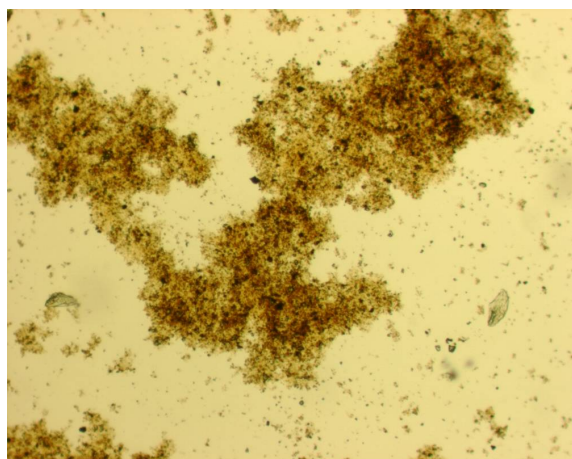
In this research, fayalites, which total weight is about 10g, are put in the test tube filled with distilled water. The diameter of these fayalites is about 3mm~5mm. They are grain shaped and the color is dark green. The test tube is irradiated with ultraviolet rays with their peak wave length of 254 nm. Another experiment was done as a comparison under the same condition but without ultraviolet. The tubes were irradiated with ultraviolet rays for three months. The illuminance of ultraviolet rays is 40w/m² when the experiments were first started.

As a result of this experiment, a lot of light brown powder was generated in both of the test tubes that were irradiated with ultraviolet rays. However, the tube without ultraviolet rays' irradiation generated less powder. Therefore, we can conclude that irradiation of ultraviolet rays causes larger amount of the powder. From the result of EPMA analysis, the powder is the amorphous iron oxide hydroxide.

Moreover, we can estimate that ultraviolet rays might promote the oxidization of fayalites in the water. It is presumed that water existed in the past on Mars' surface.

I think that there is a possibility on the Mars' surface that the rocks contained fayalites were oxidized by the water and ultraviolet rays.

Keywords: ultraviolet rays, water, fayalite, iron(III) oxide hydroxide., Mars



Difference on tectonics and rheological structure of Venus and Earth inferred from deformation experiments

AZUMA, Shintaro^{1*}, KATAYAMA, Ikuo¹, NAKAKUKI, Tomoeki¹

¹Department of Earth and Planetary Sciences System, Hiroshima university

Venus has been regarded as a twin planet to the Earth, because of density, mass, size and distance from the Sun (Taylor and McLennan, 2008). However, the Magellan mission revealed that plate tectonics is unlikely to work on the Venus (Turcotte et al., 1999). The plate tectonics is one of the most important mechanism of heat transport and material circulation of the Earth, consequently, its absence might cause the different tectonic evolution between Earth and Venus. Rheological structure is a key to inferring mantle structure and convection style of planet interiors because the rock rheology controls strength and deformation mechanism. In previous study, the behavior of Venusian lithosphere has been inferred from the power-law type flow law of dry diabase (Mackwell et al., 1998). They indicated that lower crust can be weaker than upper mantle, which might result decoupling at the crust-mantle boundary (Moho depth) and mantle convection without crustal entrainment. However, the power-law creep cannot be applicable to infer the rheological structure at Moho depths, because the dislocation-glide control creep (Peierls mechanism) is known to become dominant at relatively low temperatures in materials with a relatively strong chemical bonding such as silicates (Tsenn and Carter 1987). In this study, we conduct two-phase deformation experiments to directly investigate rheological contrast between plagioclase (crust) and olivine (mantle) using solid-medium deformation apparatus and discuss the difference between these planets in terms of rheological behaviors.

In this study, we performed experiment to directly determine the relative strength between plagioclase and olivine without any extrapolating of flow law; the crustal materials consist predominantly of plagioclase that largely control deformation of the crust, whereas deformation of the upper mantle is largely controlled by olivine. These samples are together sandwiched between alumina pistons in a simple shear geometry and we used the hot-pressed samples and performed deformation experiments using solid-medium deformation apparatus. The experimental conditions were ranging 1GPa and 600-1000 degrees, corresponding conditions approximately to Moho of the Venus under dry conditions.

The experimental results under dry conditions show that olivine is expected to always be stronger than plagioclase. The rheological structures of Venus are inferred from our experimental results and draw a comparison between Earth and Venus. In case of the Earth, rheological structure of oceanic lithosphere is constrained well by Byerlee's law and power-law type flow law (e.g., Kohlstedt et al., 1995). The moho of oceanic lithosphere is still brittle deformation range owing to the low temperature. The oceanic crust and mantle lithosphere are strongly coupled mechanically, so that they could move and subduct together into the deep. The temperature of moho, which strongly influences the coupling strength, depends on crustal thickness. The crustal thickness of Venus is, however, not constrained by the observation. In this study, crustal thickness of Venus is assumed to be 7km because of comparison with oceanic lithosphere of the Earth. Our experimental results imply that large strength contrast exists between lower crust and upper mantle in Venus. Decoupling of the motion between the crust and mantle lithospheres is expected to occur because the weak lower crust acts as a lubricant. Moreover, the soft crust cannot subduct into the hard mantle. The strength contrast between the crust and the mantle is supposed to prevent from recycling the crust into the mantle as Earth's plate tectonics. To quantitatively examine the effects of the soft lower crust on the Venusian tectonics, we are conducting numerical simulation using the rheology obtained from our experiments.

Keywords: plagioclase, olivine, strength contrast, venus, rheology, plate tectonics

An highly accurate semi-analytical EOS along Hugoniot curves

SUGITA, Seiji^{1*}, KUROSAWA, Kosuke², KADONO, Toshihiko³, SANO, Takayoshi³

¹University of Tokyo, ²JAXA/ISAS, ³Osaka University

Recent rapid development of shock compression technology has revealed many exciting properties of geologic materials under highly shock-compressed states. A number of very sophisticated thermodynamics-based equations of state (EOS), such as SESAME and M-ANEOS, have been developed. These numerical EOS codes, however, use many model parameters to reproduce experimental data. Thus, it is difficult to find the optimum model parameters uniquely, requiring extensive experiments covering a wide range of thermodynamic conditions.

Such complex EOS's have widely been considered necessary because physics behind the EOS of highly shock-compressed geologic materials is very complicated. In fact, recent experimental result using high-power laser have revealed further intricate properties of silicates under high compression conditions, such as large departure of isochoric specific heat C_v from Dulong-Petit limit due to molecular dissociation and ionization. In order to incorporate such complex properties into a thermodynamics-based EOS properly, physics behind these materials needs to model well.

Such thorough understanding of material properties is essential for building a versatile EOS for hydro-code calculations. However, many planetary applications requires only thermodynamic properties along Hugoniot compression curve. For example, estimation of the fractions impact melt/vapor and the final molecular composition of impact vapor plume requires only the entropy gain due to initial impact shock. In this study, we propose a semi-analytical formula of on-Hugoniot EOS derived from the differential form of Rankine-Hugoniot equation and compare it with conventional EOS's and experimental data.

Most condensed matter under shock compression is known to follow the linear velocity relation between particle velocity U_p and shock velocity U_s :

$$U_s = C_0 + s U_p, (1)$$

where C_0 , and s are bulk sound velocity and a constant, respectively. This relation is known to hold for a variety of materials over a wide range of impact velocity. Despite the wide applicability of this relation, most EOS's do not take advantage of this relation. Besides the U_p - U_s relation (1), we use only general thermodynamic relations, the differential form of Rankine-Hugoniot relations, and Gruneisen EOS. From these relations, we obtain ordinary differential equations for temperature T and entropy S .

For extremely high-pressure shocks, C_v is not approximated by a constant value well; it may become well above Dulong-Petit limit. The effect of specific heats can be calculated easily with our new EOS. Although there is good agreement among different EOS's at relatively low shock pressures (~ 150 GPa), different EOS's yield significantly different results at higher shock pressures (several hundred GPa). This scatter results from the fact that there are not many experimental data available in the higher shock pressure range. Under such conditions, our EOS is useful because it does not require many data points to make accurate predictions along a Hugoniot curve. It can also be used as an anchor for the more sophisticated EOS for Hugoniot conditions.

Furthermore, because C_v is a very important property to characterize condensed matter, the capability to derive C_v from temperature data is very useful. A couple of examples of comparisons between our recent experimental data and our EOS predictions are obtained. The quartz data at 150 GPa requires C_v significantly larger than 3R, but the shock temperatures of diopside at ~ 300 GPa is consistent with the Dulong-Petit value. Such difference in C_v among different silicates is of great importance in planetary science.

Keywords: shock compression, High pressure EOS, hypervelocity impact

How impact flashes differ between rocky impactors and icy impactors

YANAGISAWA, Masahisa^{1*}

¹Univ. Electro-Communications

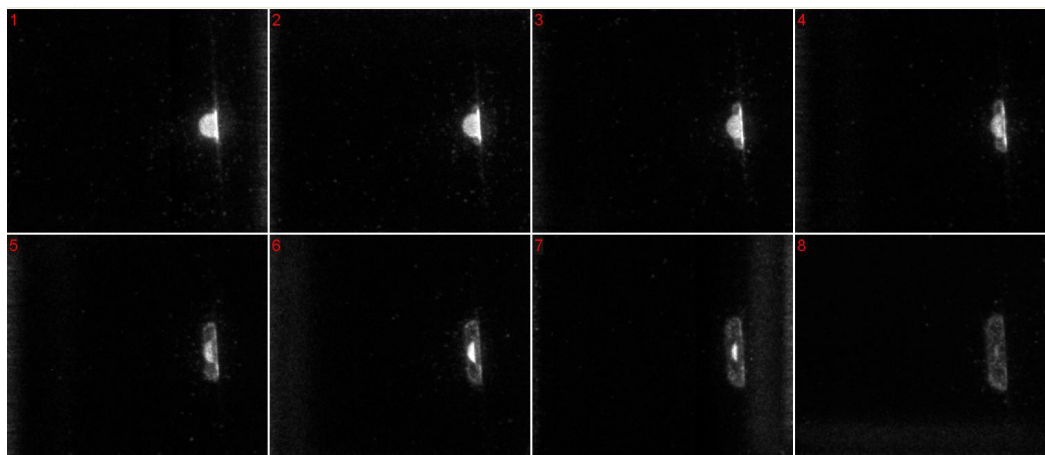
Impacts at velocities of several km/s generate luminous flashes. We conducted the laboratory impact experiments to study the characteristics of the impact flashes as follows;

- (1) impact velocity: 7km/s,
- (2) projectile: nylon 66 sphere (7mm in diameter),
- (3) target: nylon 66 block (8cm x 8cm x 4cm),
- (4) impact angle: normal impact,
- (5) instruments: photo diodes and an ultra-high speed camera (nac ULTRA Neo).

The photo diode signals for each shot show an optical pulse, the duration of which is equal to the [projectile diameter/impact velocity]. The camera images corresponding to the pulses show glowing projectiles and the target surface near the impact point (see the figure for example, shot1545). The 8 frames from left to right and top to down of the figure are obtained every 50ns (the exposure time is also 50ns). The radiation from the high temperature and the high pressure region due to the shock compression is observed through the translucent nylon projectile and target. The existence or no existence of the optical pulse may be used in the observations of the planetary impact flashes to discriminate the icy meteoroids (translucent) from the rocky meteoroids (opaque).

This research was supported by the Space Plasma Laboratory, ISAS/JAXA. The ultra-high speed frames in the figure were taken by the nac Image Technology Inc..

Keywords: high velocity impact, impact flash, small solar system objects



Physical Process on Penetration of High Velocity Dusts Captured by Very Porous Small Bodies

OKAMOTO, Takaya^{1*}, NAKAMURA, Akiko¹, KUROSAWA, Kosuke², HASEGAWA, Sunao², IKEZAKI, Katsutoshi³, TSUCHIYAMA, Akira³

¹Department of Planetary Science, Graduate School of Science, Kobe University, ²Institute of Space and Astronautical Science, JAXA, ³Department of Earth and Space Science, Graduate School of Science, Osaka University

Through the evolution of the Solar System, dusts collided with each other to become primitive bodies. Such dusts are the original components, i.e. building blocks, of the bodies. Small porous bodies can also contain exotic components because they might have captured dusts which were once located in regions of different heliocentric distances and were eventually transported to the bodies. Large flux of the exotic dusts can modify the structure and composition of the surface.

The purpose of this study is to examine the physical processes, such as the penetration depth, the degree of dust fragmentation, the morphology of the track, when high velocity dusts penetrate into very porous small bodies. Dust penetration processes into silica aerogel has been intensively studied for the calibration of the Stardust tracks (Horz et al.2006 etc). However, it is not clear how far those understandings for dust penetration into aerogel can be extrapolated to dust penetration into porous small bodies in planetary systems. In order to get better understanding of the physical processes of dust penetration into porous small bodies, we conducted impact experiments of porous sintered glass targets with different porosities and impact velocities.

We prepared three different targets, fluffy 94, fluffy 87 and fluffy 80. Hollow glass microspheres, which are composed of soda lime borosilicate glass were sintered in a cylindrical mold at different condition to have bulk porosities of 87 and 94 %. Low alkali glass particles were also sintered to have 80% bulk porosity. The typical target length was about 130 mm.

Impact experiments were performed using a two-stage light-gas gun at ISAS, JAXA. The projectiles were Ti, Al and Stainless spheres of 1 and 3.2 mm in diameter, and basalt cylinder of 3.2 mm in diameter and 2.0 mm in height. The impact velocity was ranged from 1.7 to 7.2 km/s. We observed the deceleration process of the projectiles using a flash X-ray imaging system and a high-speed framing camera. The track morphology of the targets and the degree of the projectile fragmentation were observed using ELE-SCAN (an instrument for X-ray tomography) at Osaka University and got transmission images.

The 1 mm projectiles were captured by the targets, while the 3.2 mm projectiles disrupted the targets. Images by flash X-ray with time interval show the growth of the track and disruption of the projectile in the targets. The deceleration of the projectile was analyzed using the fluid drag equation in which the drag is proportional to the projectile velocity, drag coefficient, target bulk density, the cross sectional area of the projectile and square of velocity. We fixed the projectile mass and cross section to those of the initial value. However, in general, they change during penetration. We obtained the result of the drag coefficient which increased monotonically with the initial dynamic pressure. This agrees with the increase of the ratio of the cross sectional area to the mass of the projectile due to mass loss and the shape-change of the projectiles.

The track was long and thin, called as carrot-shape, when the projectile was intact, while it was short and thick, called as bulb-shape, when the projectile was fragmented. This is similar to the track of aerogel formed by dust penetration.

The volume of the track increases with the projectile kinetic energy. Such behavior was observed for dust penetration into foamed polymers (Kadono 1999). The mass of the track is proportional to the projectile kinetic energy when the terminal projectile is still large.

In this presentation, we discuss a model of penetration depth. Niimi et al. 2011 presented a model for penetration depth of a carrot-shape aerogel track. This model assumes that drag is proportional to the square of velocity when projectile has high velocity, while it is proportional to the strength of the target when it is low velocity. We modify this model to fit the result of our experiments.

Keywords: Porosity, Small bodies, Flash X-ray, Deceleration

Experimental Study on Momentum Change of Porous Small Bodies by Collisions

AOKI, Takanobu^{1*}, NAKAMURA, Akiko¹, OKAMOTO, Takaya¹, HASEGAWA, Sunao²

¹Graduate School of Science, Kobe University, ²Japan Aerospace Exploration Agency

Non-gravitational effects that can affect the orbital motion of small bodies include electromagnetic effects such as Yarkovsky effect as well as mutual collision. It is therefore very important to know the degree of momentum change of a small body when it is collided by smaller objects. The ratio of the momentum that a target has after a collision to before is called momentum transfer efficiency. Laboratory impact experiments on momentum transfer have previously been performed. One with nylon projectiles and mortar sphere targets showed the momentum-transfer efficiency exceeds unity and increases linearly with the impact velocity due to fragments ejected opposite to the projectile's trajectory (Sirono et al. 1993). The previous studies were performed for targets with less porosity, however, recent study showed that there are asteroids with high porosity, such as 253 Mathilde and 283 Emma (Baer et al. 2011). The porosity of these objects is more than 50%. Asteroid 25143 Itokawa explored by Hayabusa spacecraft has porosity of about 40% covered with boulders. Itokawa is a rubble pile object which was formed by reaccumulating fragments of disrupted parent body. After the reaccumulation event, the body may have experienced further impact events. How greatly Itokawa's orbit has changed after the reaccumulation will be better understood once the momentum transfer efficiency to porous bodies from small-mass impactor is clarified.

Therefore, we performed high velocity impact experiments using a two-stage light-gas gun at ISAS, JAXA. The projectiles are Aluminum and Titanium spheres of 1 and 3.2 mm in diameter. The targets are cylinders of sintered glass beads of different porosities and sea sand filled in a plastic container. The porosity of these targets are 40~93 %. We suspended each target with two strings, and impacted a projectile at up to 7.5 km/s. We used three high-speed framing cameras. The preliminary results show that the ejecta can carry tens of % of the projectile momentum similarly to those found for lower porosity targets in previous studies.

Keywords: porosity, asteroid, impact, orbit

Low-velocity impact experiments on equal-sized planetesimal collisions

KOMOTO, Yasunari^{1*}, YASUI, Minami², SHIMAKI, Yuri³, ARAKAWA, Masahiko¹

¹Graduate School of Science, Kobe University, ²Organization of Advanced Science and Technology, Kobe University, ³Graduate School of Environmental Studies

Planets in the solar system have grown by mutual collisions among porous planetesimals. The Hayashi model suggested that many equal-sized planetesimals depending on the heliocentric distance were formed by the gravitational instability of dusts in the solar system. Moreover, it is expected that the collisional velocities among planetesimals were equal to or larger than the escape velocity and not only a head-on collision but also an oblique collision with various impact angles occurred. In this study, we conducted oblique impact experiments with low-impact velocity for samples simulating rocky and icy planetesimals and examined the effects of composition and impact angle on the impact strength and fragment velocity.

We prepared projectiles and targets of polycrystalline ice and porous gypsum with a porosity of 55 % simulating icy and rocky planetesimals, respectively. All samples have a spherical shape with a diameter of 30 mm. Impact experiments were conducted by an one-stage He-gas gun in Kobe University for gypsum samples and in the cold room of ILTS at -10° C. The impact velocities (V_i) were 12.5-83.3 m/s for a head-on impact and 65-75 m/s for an oblique impact. The impact angle (l) changed every 15° from 0 to 75°. The target was set in the recovery box to measure the mass of each fragment. The collisional disruption of the projectile and the target was observed by a high-speed video camera at the frame rate of 3000-8000 frames s^{-1} . We measured the antipodal velocity (V_a), which was the fragment velocity ejected from the antipodal point of the impact point on both the projectile and the target to study the effect of oblique impacts on the average fragment velocity.

We found in the case of the head-on collision that the V_a was almost consistent with the velocity of the center of mass (V_g). However, the V_a was about 10-15 m/s smaller than the V_g due to the crush of the target in the case of ice sample. Moreover, many finer fragments were ejected from the impact point in a direction perpendicular to the impact direction, and the fragment velocities became the maximum as same as the impact velocity. In the case of oblique impacts, the V_a decreased with the increase of the l . The fragment velocity ejected from the impact point to the tangential direction of impact surface was about 1.5 times larger than the V_i due to jetting in the downstream while it was more than two times smaller than the V_i in the upstream. The relationship between the V_a and the l could be written by $V_a=20(\cos l)^{3.6}$ for the ice target of $l=0-45^\circ$, $V_a=7.7(\cos l)^{0.95}$ for that of $l=45-75^\circ$, and $V_a=31(\cos l)^{1.3}$ for porous gypsum. We notice that in the cases of $l=45-75^\circ$, the power law index of $\cos l$ was almost 1 and the maximum fragment mass normalized to the original sample mass m_l/M_p or $t (=M)$ was about 0.5-1.0.

In the case of head-on impacts, the Q^* for ice was 89 J/kg at the mass ratio of projectile and target M_p/M_t of 0.003-0.13 obtained by Arakawa et al. (1995) and Arakawa (1999), and the Q^* for porous gypsum was 446 J/kg at the M_p/M_t of 0.027-0.56 obtained by Yasui and Arakawa (2011). In this study, the Q^* of ice and porous gypsum samples were almost consistent with those obtained by these previous works. In the case of oblique impacts, the m_l increased with the l , and the relationship between the m_l/M and the l could be written by $m_l/M=0.044(\cos l)^{-1.4}$ for ice and $m_l/M=0.44(\cos l)^{-0.62}$ for porous gypsum. Moreover, it is suggested that the normal component of impact velocity to the tangential surface at impact point ($V_i \cos l$) had the significant effect on the m_l/M so we reanalyzed the data by using the $Q(\cos l)^2$. As a result, the results for head-on impacts were almost consistent with those for oblique impacts, that is, we succeeded to scale the effect of impact angle on the m_l/M .

Keywords: Oblique impact, Planetesimals, Porous body, Icy body

Shock-induced devolatilization from calcite in an open system using a two-stage light gas gun

KUROSAWA, Kosuke^{1*}, OHNO, Sohsuke², SUGITA, Seiji³, Tetsu Mieno⁴, MATSUI, Takafumi², HASEGAWA, Sunao¹

¹ISAS, JAXA, ²PERC, Chiba Institute of Technology, ³Graduate School of Frontier Science, The Univ. of Tokyo, ⁴Faculty of Science, Shizuoka Univ.

We investigated shock-induced decarbonation of non-porous calcite in an open system at a wide range of peak shock pressures using a two-stage light gas gun and a quadrupole mass spectrometer. A new experimental technique that avoids chemical contamination from the acceleration gas from the gun was developed. We also conducted high-speed imaging and spectroscopic observations simultaneously to investigate the validity of our experimental procedure. We newly found that the decarbonation efficiency along the Hugoniot curve changes around 50 GPa, which is close to the predicted pressure for incipient decarbonation by ANEOS. Although shock-induced decarbonation was detected at the pressure lower than 50 GPa as well as the previous experimental studies, decarbonation may be caused by local energy concentration due to shear banding, resulting in low decarbonation efficiency. We constructed a simple theoretical model for shock-induced decarbonation during isentropic release based on the entropy method and the lever rule under our experimental condition. The predicted CO₂ amount as a function of peak shock pressure agrees well the experimental results at >50 GPa, strongly suggesting that the shock-induced CO₂ amount is determined only by the entropy for the peak shock state, incipient and complete decarbonation at the ambient pressure. We can use the new method for the quantitative measurements of the chemical composition of impact-induced gases from solid materials without any modification. The new technique is very useful to investigate the required peak shock pressure for vaporization/devolatilization of geologic materials and the final chemical composition in impact-induced vapor clouds.

Keywords: Impact-induced devolatilization, Gas-phase chemical analysis, Open system, Two-stage light gas gun, Mass spectrometry, Carbonate

Analyses of Planar Deformation Features (PDFs) of Shocked Quartz Grains Derived from K-Pg Boundary Deposits within and o

CHANG, Yu^{1*}, TAJIKA, Eiichi², GOTO, Kazuhisa³, SEKINE, Yasuhito²

¹Earth and Planetary Sci., Univ. of Tokyo, ²Complexity Sci. & Eng., Univ. of Tokyo, ³Chiba Institute of Technology

Impacts of extraterrestrial objects on the Earth have played a major role in the origin and evolution of the Earth and life. Impact processes on the Earth with thick atmosphere are, however, not precisely understood because of lack of detailed study on the distribution of ejecta around the large impact craters on the Earth.

One of the largest impact structures on the Earth is the Chicxulub Crater, Yucatan Peninsula in Mexico, which caused the mass extinction event at the Cretaceous-Paleogene (K-Pg) boundary at 65 million years ago. The details of impact processes of the Chicxulub crater is, however, largely unknown.

In this study, we measured and analyzed planar deformation features (PDFs) on shocked quartz grains derived from asteroid impact at the K-Pg boundary deposits both within the Chicxulub crater (Yaxcopoil-1 site) and outside of the crater (K-Pg boundary tsunami deposits in western Cuba) in order to reveal processes in the large asteroid impacts on the Earth. PDFs are planar micro structures generated under high-pressure condition (5~30GPa) and crystallographic orientation is known to vary with shock pressure. The samples are collected from seven vertical levels of the Yaxcopoil-1 drilling core within the Chicxulub crater. We investigate the characteristic features of the ejection and deposition of shocked quartz grains with various pressure level of PDFs by comparing the samples within the crater with the samples from proximal ejecta around the crater.

Keywords: shocked quartz, K-Pg boundary, planar deformation features (PDFs), impact crater, ejecta

Fragmentation Degree of Impactor in Collision between Asteroids

NAGAOKA, Hiroki^{1*}, NAKAMURA, Akiko¹, SANGEN, Kazuyoshi¹

¹Graduate School of Science, Kobe University

Introduction

Many of meteorites are fragments of disrupted asteroids, and we can get the information of early stages of the Solar System, because it is considered that thermal activity was stopped in the early stage in the parent bodies of chondrites. Meteorites are classified according to their parent bodies and chemical composition. However, there are meteorites in which the components from various parent body origins are mixed. About 20 % of ordinary chondrites have brecciated. Brecciated meteorites were probably formed by impacts of smaller bodies into boulders or regolith of another bodies and being captured in the regolith (e.g. Rubin et al. 1983).

In this study, we assumed that a meteorite impacts into regolith, and the fragments are captured in regolith. We aimed to clarify fragmentation degree of projectile.

Experiments

Projectiles simulating meteorites are impacted on regolith like sand targets at velocities of 167 to 429m/s. The samples used as projectiles were pyrophyllite cylinders and as targets were silica sand. The impact experiments were performed mainly by a single-stage powder gun facility at the department of Science, Kobe University. Recovered fragments were sorted out by 0.5mm size meshes.

Results

We studied that the relation of the largest fragment mass to impact energy density (in this study, it was defined as the kinetic energy of the projectile per unit mass of the projectile) and the peak pressure. It was found that projectiles began to break at 10^4 J/kg in kinetic energy density, and this is large by two orders of magnitude when compared with the value of the previous experiment (Takagi et al. 1984) with larger targets. Projectiles began to break at initial pressure of 300 MPa, and this is larger than the compressive strength of pyrophyllite.

We will conduct experiments on the influence of the difference in rock material as projectiles and the particle diameter of sand as targets, and discuss on the results.

Keywords: asteroid, meteorite, impact

Experimental investigation of parameter dependence for thermal conductivity of regolith

SAKATANI, Naoya^{1*}, OGAWA, Kazunori¹, Yu-ichi Iijima¹, HONDA, Rie², TANAKA, Satoshi¹

¹Institute of Space and Astronautical Science, ²Kochi University

Moon, Mercury, or asteroids' surface is covered with regolith. Thermal conductivity of powder material as regolith under vacuum environment depends on several parameters such as particle size, porosity, temperature, and stress. Although lunar thermal conductivity was measured in Apollo Heat Flow Experiments, the measured thermal conductivity seems to differ from the original one due to change in the regolith condition during drilling (Langseth et al., 1976). For correction of the measured thermal conductivity and for in-situ heat flow measurements in future, it is required to quantify the thermal conductivity variation as a result from the change of the regolith condition. Furthermore, powder materials have extremely low thermal conductivity of an order of 0.001 W/mK under vacuum condition. Therefore regolith layer on small bodies behaves as a heat-insulating layer, which affects their thermal evolution (Akridge et al., 1998). Since regolith condition on the small bodies which are under low gravity has uncertainty, it will be required that the thermal conductivity is modeled and its range is restricted. The purpose of this study is that the parameter dependencies of powders' thermal conductivity are investigated experimentally under vacuum condition and the heat transfer mechanism is understood.

The powders' thermal conductivity under vacuum is represented as sum of two contributions; thermal conduction through the particle contact region (solid conductivity) and thermal radiation between adjacent particle surfaces (radiative conductivity). One of the methods for separation of measured conductivity into these two conductivities is to investigate temperature dependence of the thermal conductivity assuming the temperature dependence of the radiative conductivity (Watson, 1964). Merrill (1969) studied the particle size dependence of the solid and radiative conductivities using some sizes of glass beads according to the Watson's method. The solid conductivity decreased with increasing the particle size, which was explained by the number of contact points of thermal resistances per unit volume. The radiative conductivity increased with the particle size, which was interpreted as making the effective length between particles longer. However, the glass beads he used had large porosity variation among the sample sizes, and therefore, his result might not reflect only the particle size effect, which will cause misunderstanding of the heat transfer mechanism. In this presentation, we re-investigated the particle size effect on the solid and radiative conductivity using several sizes of glass beads with porosity being almost constant among the sizes.

We used five sizes of glass beads, which have almost constant porosity. The thermal conductivity was measured by the line heat source method. The system's temperature was controlled by a thermostatic chamber from -25 to 50 degC. The thermal conductivity was separated into solid and radiative conductivities according to the Watson's method.

The results were the followings. The radiative conductivity increased linearly with increasing the particle size, consistent with the Merrill's result. On the other hand, the particle size dependence of the solid conductivity was different from Merrill's, which would reflect the effect of the porosity control; the solid conductivity slightly increased with increasing the particle size. Our results can be interpreted as not only (1) the effect of the number of contact points per unit volume but also (2) the effect of the particle size on thermal conductance per unit contact region. In theoretical model including these two effects (Halajian and Reichman, 1969), the solid conductivity is independent of the particle size, and it was found that the theoretical model derives comparable value with the solid conductivity obtained in this study.

Keywords: regolith, thermal conductivity

Development of the extending probe for lunar and planetary heat flow measurement

HORIKAWA, Yamato^{1*}, Satoshi Tanaka², Kazunori Ogawa², Taizo Kobayashi³, Akio Fujimura²

¹Tokyo University, ²Japan Aerospace Exploration Agency, ³Fukui University

The heat flow measurement in the lunar and planetary surface layers is an important method which constrains their internal activity, thermal history and material composition. In the case of the Moon, the internal heat source would be mostly radioisotopes, which are also refractory elements and elements concentrated in melt. Therefore the heat flow measurement constrains bulk quantity and distribution of radioisotopes, and they are essential for the verification of the giant impact theory and the magma ocean theory. The in-situ measurements were conducted in the Apollo 15 and 17 missions. But because a part of the heat flow probe was exposed on the lunar surface, and the measurements are also influenced by the thermal difference during day and night on the surface, the correct heat flow values could not have been measured. Penetrating probes including penetrators would not be exposed on the surface, but because the thermometers and heaters on the penetrating probe are exposed on the regolith, and influenced by the regolith consolidated by penetrating and the thermal distribution of the regolith varies from the heat conduction of the penetrating probe, it is difficult to determine the primary heat flow value of the planet precisely.

In this study, we propose that after the thin extending probes including a thermometer and heater are extended from both sides of the penetrating probe, they measure temperature and thermal conductivities at a point distant from the penetrating probe. By this new method, we do not have to correct the heat flow values with the physical state variation of regolith by penetration. Moreover the extending probes can measure the absolute value of thermal conductivities, and greatly enhance the accuracy to decide the heat flow values. Additionally the extending probes can explore geology and life under the surface layer if fiberglass rods are extended from the penetration probe, open at the end, and do spectral analysis.

Developing the extending probe, we especially discuss its length, diameter, and material.

We determine the shortest distance from a side of the penetrating probe to the area of the primary thermal gradient as the length of the extending probe by estimating the thermal variation of regolith after penetrating and analyzing the numerical simulations based on a thermal mathematical model of the penetrating probe. Of course the extending probes are stored inside the penetrating probe before measurement, so it can be difficult to emplace and extend the extending probes depending on their length. We discuss not only each length of extending probes but also the way to emplace and extend them.

The diameter of the extending probe should be as small as possible. This is because the error of thermal conductivities of the extending probe is reduced preferably when measuring the thermal conductivities with the line heat source method. It is also important because the extending force is reduced. But if the extending probe is made too thin, it can bend due to variation in the physical properties of regolith. We conduct penetration tests with a consolidated regolith simulant, and set out a minimum diameter required to avoid bending.

The material of the extending probes is generally stainless. But if it can not be put in the penetrating probe, we use hyperelastic material or memory metal as the material of the extending probes which can be transformed and emplaced. Additionally we have to measure the mass and thermal conductivity of the material, and choose one whose mass and thermal conductivity are as small as possible.

On this presentation, we report the current progress of analysis, experiment, and development of the extending probe.

Keywords: heat flow, moon, planet, regolith

Spectral Atlas with Hokkyodai Spectrograph on 1.6 m Pirca Telescope at Nayoro Observatory.

SEKIGUCHI, Tomohiko^{1*}, KAWAKITA Hideyo², WATANABE Makoto³

¹Hokkaido University of Education, ²Kyoto Sangyo University, ³Hokkaido University

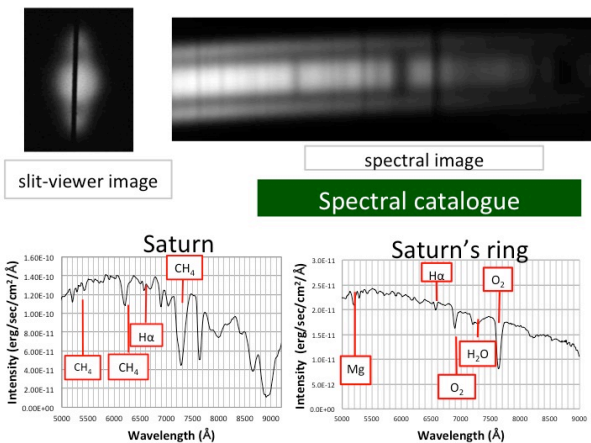
We here report on a spectroscopic atlas of solar system objects using the Hokkyodai spectrograph on the 1.6 Pirca telescope of Hokkaido university at the Nayoro observatory.

Spectroscopic observations in visible wavelength were performed with a new spectrograph in 2011.

The wavelength range of the spectrograph is from 500 nm to 900 nm, the wavelength resolution is $R > 300$. We obtained the spectroscopic data of planets: Mercury, Venus, Mars, Jupiter, Saturn, Neptune; Comet: C/2001 P1 Garrad; asteroid: 15 Eunomia in addition to the astronomical data of stars of each spectral type, several emission-line nebulae and a galaxy. One of aims of this spectral catalogue is a visualization and archive for education.

We summarize the results on the first report in 2011.

Keywords: observations, spectroscopy, spectrograph, visible wavelength



Orbital evolution of solar system bodies due to dark matter haloes and giant molecular clouds

SUZUKI, Takayuki¹, HIGUCHI, Arika^{1*}, IDA, Shigeru¹

¹Department of Earth and Planetary Science, Graduate School of Science and Technology, Tokyo Institut

We have investigated the effect of gravitational perturbations from dark matter haloes on Oort cloud comets, which are the most loosely bounded bodies among the solar system bodies. Oort cloud comets receive perturbation from external bodies: the galactic disk, nearby stars, and giant molecular clouds. The effects of these external perturbations have been studied by previous authors. Recent N-body simulations have revealed that dark matter particles form spherical-shape substructure called “dark matter halo”. Giant molecular clouds are also supposed to perturb solar system bodies. It is predicted that the dark matter haloes have a broad size distribution ranging from galactic size down to solar system size and each size equally contribution to the total mass of the galactic dark matter, in contrast to molecular clouds that are dominated by the largest bodies and nearby stars that are essentially point-like bodies. Here, we develop a formulation to evaluate the effect from external bodies with arbitrary sizes, which can be applicable for all of nearby stars, molecular clouds, and dark matter haloes. We evaluated the strength of the perturbations by dark matter haloes and giant molecular clouds by the increase rate of velocity dispersion of the solar system bodies. We found that the effect of nearby stars is generally largest, since the size distribution of dark matter haloes may include large uncertainty, we also study the parameter range in which the effect of dark matter haloes is dominated.

Keywords: Comet, Oort cloud, Trans-Neptunian objects, Giant molecular cloud, Dark matter halo

Self-gravity wakes in dense planetary rings

FUJII, Akihiko^{1*}

¹University of Tokyo

Planetary rings are composed of a number of colliding icy particles. Interplay among collisions, mutual gravitational attraction and the Keplerian shear leads to the formation of spatial structure called as "self-gravity wakes" that are prevalent throughout dense planetary rings. One can observe similar wake-like patterns in collisionless gravitational many-body systems such as galactic disks as well, which demonstrates that self-gravity wakes are a common feature among gravitationally interacting astrophysical disks.

The shapes of self-gravity wakes in diverse types of disks are different, according to the physical characteristics of the disk(disk mass, energy dissipation rate, inter-particle gravity compared with tidal force, etc). However so far no previous studies have focused on the effects of the physical properties of disks on the shape of self-gravity wakes. In order to tackle this subject for the first time, we have developed a numerical code that can deal with a sufficiently large number of self-gravitating particles within realistic CPU time, and have systematically studied the dependence of the shapes of self-gravity wakes on several physical parameters that characterize various types of particulate astrophysical disks. With the aid of a special-purpose computer GRAPE-DR, we can boost up
the computational speed.

In this study, three parameters were adopted to characterize dense planetary rings, namely, (i) the dynamical optical depth, (ii) the coefficient of restitution, and (iii) the ratio between the Hill radius and the physical radius of a ring particle. The shape of self-gravity wakes is analyzed with two-body correlation function, and the inclination (the pitch angle) of self-gravity wakes towards the orbital direction were investigated. We have found that the inclination increases with the optical depth and the ratio between the Hill radius and particle radius, but that the inclination barely depends on the coefficient of restitution. We discuss the physical mechanisms leading to these numerical results.

Keywords: planetary rings, self-gravity, Local N-body simulation

Distribution of element abundances within achondrites

NESS, Peter^{1*}, Hideaki Miyamoto¹

¹The University of Tokyo

Our understanding of the history of the solar system relies heavily on the analysis of meteorites. Many meteorites that fall to earth are achondrites, which are derived from the moon, mars (shergottites, nakhlites, chassignites) or from asteroid parent bodies (eucrites, howardites, diogenites, ureilites, iron meteorites etc). The chemistry and petrology of the different chemical groups of achondrites is known to differ substantially, which raises the question as to whether there are also major chemical differences within each/any of the various achondrite chemical groups.

To help answer this question we utilized a database that we compiled from meteorite element abundances and terrestrial from peer-reviewed papers, building on existing published databases [1-4]: we then used element abundances from these databases to analyze the major, minor and trace elements chemistry of achondrites. The meteorite database comprises 28,742 bulk chemical abundances from 2,112 meteorites compiled from 121 peer-reviewed papers published between 1953 and 2010: representing 78 atomic elements, 20 major chemistry analyses and a wide range of petrologic and chemical types. The terrestrial database comprises 71,245 bulk chemical abundances compiled from 2,848 rocks, from 66 peer-reviewed papers published between 1982 and 2011.

The results of our analysis suggest that there is no significant difference in major chemistry of most meteorites within the majority of achondrite groups. However, there can be significant differences in major chemistry for aubrites and iron meteorites. We also find that lodranites, aubrites and some meteorites from the moon and mars can also contain anomalous metal and trace elements. These anomalous element abundances often differ by many times the mean of their particular achondrite group, which might suggest that metals and other atomic elements have been injected/ depleted by hydrothermal/alteration or by other processes.

We found it difficult to analyze the major chemistry of iron meteorites due to a lack (absence) of major chemical abundances. Given that most iron mines on Earth use major chemistry for rock/material type interpretation we recommend a concerted effort to obtain better coverage of the major chemistry of iron meteorites.

The implication of this research is that a potential might exist for finding metal and trace element resources on the moon, mars, or even on some asteroid parent bodies.

Keywords: meteorites, achondrites, element abundances, distribution, major chemistry

Shock-wave decay and shock metamorphism of laser-shocked minerals

NAGAKI, Keita¹, SAKAIYA, Tatsuhiro^{1*}, KONDO, Tadashi¹, KADONO, Toshihiko², Youichirou Hironaka², SHIGEMORI, Keisuke²

¹Graduate School of Science, Osaka Univ., ²ILE, Osaka Univ.

It is important to recover the shock-compressed samples for understanding the synthetic mechanism of high-pressure phase, shock metamorphism and shock-melt vein in meteorites. In the past, many impact experiments have conducted by using explosive or gas guns. In fact, although high-pressure phase in meteorites is recovered by the impact experiments (impact velocity is 1.5km/s and shock pressure is 26GPa) [1], the impact velocity in these methods is limited below 10km/s less than second escape velocity on the Earth. Recently, impact experiments at the velocity over 10km/s were conducted by using projectiles which were accelerated by high-power laser [2].

We developed the recovery technique of the laser-shocked materials at higher pressures (130-460GPa) in high-power laser system and estimated the pressure range of the production conditions from analyzing the structure of the shock metamorphism. We used the single crystal olivine (from San Carlos, USA) which is a major mineral of meteorites and of the Earth. We used the aluminum recovery cell. On this cell, titanium plate was located in the front of olivine to prevent the sample from being blow off. We used GXII/HIPER laser system at Institute of Laser Engineering (ILE), Osaka University [3]. The deformation, fracture and phase identification of the recovered olivine were observed comprehensively by optical microscopy, field emission-scanning electron microscopy (FE-SEM), electron backscatter diffraction (EBSD) and micro-Raman spectroscopy.

We recovered about 100 wt.% of the sample. There were some distinctive structures in the recovered sample. We estimated the shock wave attenuation rate from the distribution of these structures. The attenuation rates were 2.2-2.9 in our experiments. These attenuation rates were larger than that in previous experiment [4] and simulations [5, 6].

Part of this work was performed under the Joint Research of Institute of Laser Engineering, Osaka University.

References

- [1] Tschauner, O. et al., Proceedings of the National Academy of Sciences, 106, 13691-13695, 2009.
- [2] Kadono, T. et al., Journal of Geophysical Research, 115, E04003, 2010.
- [3] Yamanaka, C. et al., Nucl. Fusion, 27, 19-30, 1987.
- [4] Nakazawa, S., et al., Icarus, 156, 539-550, 2002.
- [5] Ahrens, T. J., and J. D. O'Keefe, Int. J. Impact Eng., 5, 13-32, 1987.
- [6] Pierazzo, E., et al., Icarus, 127, 408-423, 1997.

Keywords: Shock wave, Metamorphism, Olivine, Laser, Recovery, Experiment

Analysis of volatile components and recovery samples of laser-shocked Murchison meteorite

NAKABAYASHI, Makoto^{1*}, YABUTA, Hikaru¹, SAKAIYA, Tatsuhiro¹, KONDO, Tadashi¹, OHNO, Sohsuke², KADONO, Toshihiko³, SHIGEMORI, Keisuke³, HIRONAKA Yoichiro³, YAMANAKA, Takamitsu⁴

¹Earth and Space Sci., Osaka Univ., ²PERC, Chiba Institute of Technology, ³Inst. of Laser Engineering, Osaka Univ., ⁴Geophysical Laboratory, Carnegie Inst.

It has been suggested that organics in meteorites and comets has delivered building blocks of life to the early Earth during the late heavy bombardment [1]. However, there has remained a missing link in the subsequent chemical evolution of these small bodies via their interaction with the early Earth. Although the shock experiments have been reported by using gas gun (e.g. [2]), which is an efficient method for consideration about impacts of meteorites and comets, these are performed under a closed system at lower impact velocities due to the experimental restrictions. Recently, the shock experiments using high-power laser have been available [3] under an open system at higher impact velocities (> 10 km/s). In this study, we have conducted a laser-shock experiment for Murchison meteorite under more realistic condition of impact events in order to identify the produced volatile components that might have been contributed to abiotic synthesis of organics and chemical composition of atmosphere in the early Earth.

Finely ground Murchison meteorite, CM2 chondrite, was used as starting material. Silica powder, which did not contain organics, was also used as a standard sample. Both samples were pressed into pellets in a diamond anvil cell. The thickness and diameter of pellets were about 100 μm and about 300-850 μm respectively. The aluminum foil of 50 μm thickness was located in front of the sample as the ablator for the laser and for preventing the sample from blowing out. The laser-shock experiments were conducted using GEKKO XII/HIPER laser at Institute of Laser Engineering, Osaka University, Japan [4]. The laser wavelength, pulse duration, and spot diameter were 1053 nm, 20 ns, and 0.4 mm, respectively. The experimental shock pressures were about 400 GPa and 200 GPa. The shocked sample was recovered by aluminum box or double glass vial. The ejected volatile components were analyzed on site by quadrupole mass spectrometry (QMS). The recovered material inside of the cell was extracted in solvent, and it was analyzed by gas chromatograph mass spectrometry (GC-MS).

The produced volatiles were the components with mass numbers of 16 and 26 at 400 GPa, and of 34 at 200 GPa, which could be identified as CH_4 , C_2H_2 , and H_2S , respectively. Although small amounts of tiny solid particles have been recovered in the cell, some of them were possibly derived from aluminum foil, and it is not sure whether they are indigenous from the meteorite. No compounds were identified by GC-MS analysis of the solvent extracts of the cell. The product, CH_4 , in this study is partly consistent with the discussions by [5] that an atmosphere generated by impact degassing would tend to CO - or CH_4 - rich composition derived from the impacting bodies. These impact-induced volatiles were reducing species and might have worked effectively for abiotic synthesis of organics in the early Earth.

References

- [1] Chyba, C., and C. Sagan (1992), *Nature* 355, 125-132.
- [2] Furukawa, Y. et al. (2009), *Nature Geoscience* 2, 62-66.
- [3] Ohno, S. et al. (2011), 42nd Lunar and Planetary Science Conference 1608, p. 1752.
- [4] Yamanaka, C. et al. (1987), *Nuclear Fusion* 27, 19-30.
- [5] K. Zahnle et al. (2010), *Cold Spring Harb. Perspect. Biol.* doi: 10.1101/cshperspect.a004895

Infrasound and Seismic Observations of the Hayabusa Reentry

ISHIHARA, Yoshiaki^{1*}, HIRAMATSU, Yoshihiro², YAMAMOTO, Masa-yuki³, FURUMOTO, Muneyoshi⁴, Kazuhisa Fujita⁵

¹RISE Project, NAOJ, ²Kanazawa Univ., ³Kochi Univ. of Tech., ⁴Nagoya Univ., ⁵JAXA

The Hayabusa, the world first sample-return minor body explorer, came back to the Earth, and reentered into the Earth's atmosphere on June 13, 2010. The Hayabusa Sample Return Capsule (H-SRC) was the third direct reentry event from the interplanetary transfer orbit to the Earth at a velocity of over 11.2 km/s. The H-SRC and the H-S/C reentries are very good analogue for studying bolide size meteors and meteorite falls. We, therefore, conducted a ground observation campaign for aspects of meteor sciences. We carried out multi-site ground observations of the Hayabusa reentry in the Woomera Prohibited Area (WPA), Australia. The observations were configured with optical imaging with still and video recordings, spectroscopies, and shockwave detection with infrasound and seismic sensors. In this study, we report details of the infrasound/seismic observations and those results.

To detect shockwaves from the H-SRC and the H-S/C, we installed three small aperture infrasound/seismic arrays as the main stations. In addition, we also installed three single component seismic sub-stations and an audible sound recorder. The infrasound and seismic sensors clearly recorded sonic boom type shockwaves from the H-SRC and disrupted fragments of the H-S/C. The audible recording also detected those shockwave sounds in the human audible band. Positive overpressure values of shockwaves (corresponding to the H-SRC) recorded at three main stations are 1.3 Pa, 1.0 Pa, and 0.7 Pa with the slant distance of 36.9 km, 54.9 km, and 67.8 km (i.e., the source altitude of 36.5 km, 38.9km, and 40.6 km), respectively. These amplitudes of shockwave overpressures are systematically smaller than those of theoretical predictions. The incident vectors of the shockwave from the H-SRC at all the three arrays are estimated by F-K spectrum and agree well with predicted ones. Particle motions of ground motions excited by the shockwave from the H-SRC show characteristics of typical Rayleigh wave.

We examine the relation between amplitudes of overpressures and ground motions, and consider the transfer function. We define the transfer function as, $Z(\omega) = rV_S v_z(\omega)/p(\omega)$, where, ω is the angular frequency, p the pressure perturbation, r the density of elastic media, V_S the shear wave velocity of elastic media, and v_z the vertical ground velocity. Here the numerator represents the pressure in the elastic media. The obtained value of transfer function is ~ 2 at frequency of around 8 Hz. We try to search elastic properties of each site (r : 1300 - 1700 kg/m³, V_P : 1200 - 1700 m/s, V_S : 100 - 300 m/s) to explain the observation. The optimum values are around r of 1500 kg/m³, V_P of 1400 m/s and V_S of 150 m/s. The effective depth of air-to-ground coupling of this frequency range is very shallow and the observation sites are covered with fine soil. Therefore the estimated values are fully suitable.

Keywords: Hayabusa, shockwave, infrasound, seismic wave, air-to-ground coupling

Linear analysis of the vertical propagation characteristic of the Venus mountain wave

ANDO, Hiroki^{1*}, Yasumitsu Maezima², IMAMURA, Takeshi³, TAKAGI, Masahiro¹, Norihiko Sugimoto⁴

¹University of Tokyo, ²Nagoya University, ³ISAS/JAXA, ⁴Keio University

In the previous VEGA balloon measurements, the strong vertical fluctuations of the balloon was observed near the altitude of 55 km above the equatorial region. Young et al. (1987) suggested that these fluctuations were influenced by surface topography associated with high mountain ranges. Moreover, Young et al. (1994) suggested that mountain waves could propagate above the Venus cloud layer through the non-linear process. Recently, from the analysis of the ultra violet images taken with the VMC on board the Venus Express, Picciali et al. (2011) argued that mountain waves propagated until the top of the Venus cloud layer.

There are very few observational and theoretical studies about the Venus mountain wave. Then, it is expected that the characteristic of the vertical propagation of the mountain wave is different depending on the latitudes because the depth of the convection layer in the cloud layer and the structures of background zonal wind are different. In particular, the depth of the convection layer in the high latitude region is thicker than in the lower latitude region, thus it is questionable that the mountain wave can really propagate above the convection layer in the high latitude region. Moreover, there is no study that considers the effects of the convection in the cloud layer on the propagation of the mountain wave. Therefore, first of all, we carried out the linear calculation of the mountain wave replacing the effects of the convection with the large diffusion coefficient. In this presentation, we are going to show the result of this linear calculation and the future plan for the study by using a non-linear model.

Keywords: Venus, Mountain wave

Numerical modeling of cloud-level convection on Venus

HIGUCHI, Takehito^{1*}, IMAMURA Takeshi², TAKAGI Masahiro¹, MAEJIMA Yasumitsu³, SUGIMOTO Norihiko⁴, ANDO Hiroki¹

¹The University of Tokyo, ²Japan Aerospace Exploration Agency, ³Nagoya Univertisty, ⁴Keio Univesity

Venus is covered by clouds of sulfuric acid in the altitude region from 45 to 70km. Vertical winds that could be caused by convection were observed by Vega balloons at around 55 km altitude near the equator. The presence of neutral stratification at around 50-55km in the middle and lower clouds has been known from temperature profiles obtained by radio occultation. This suggests the existence of convective activity in this region. The convection is attributed to the heating of the cloud base by the absorption of upward thermal radiation from the lower atmosphere. Cellular structures with horizontal scales of a few hundred kilometers observed at the cloud top by the Venus Monitoring Camera onboard the Venus Express may be caused by this convection. However, the dynamical linkage between the convection layer and the cloud top, which are separated by 5-10 km, is not clear.

Baker et al. [1998] performed two-dimensional numerical experiments of cloud-level convection, which penetrates into stable layers above and below, assuming the background density and temperature profile and the net heat flux in this height region. A problem of their study would be that they represent radiative energy transport by diffusion, which is not a good approximation in the upper cloud region. Furthermore, the horizontal scales convective cells in the model are much smaller than to the cellular structures at the cloud top, and thus relationship to the cloud top feature is not fully understood. In order to understand the factors that determine the basic structure of the cloud-level convection on Venus, it is necessary to calculate convection based on more realistic radiative heating.

In this study, cloud-level convection on Venus is studied using the non-hydrostatic meteorological model CReSS [Tsuboki and Sakakibara, 2007]. The heating by shortwave radiation is the same as that of Baker et al. [1998], but the heating and cooling by longwave radiation are given in a form more realistic than the previous study. We will discuss how the structure of convection depends on the magnitude of the heating and other background parameters based on the model result.

Keywords: Venus, convection, radiation